https://doi.org/10.5194/egusphere-2025-5377
Preprint. Discussion started: 12 November 2025

DOM consumption and demethylation as potential drivers of low MeHg in Mediterranean Sea sponges and benthic fish: a modelling perspective

David J. Amptmeijer[1], Ulrike Hanz[2], Corinna Schrum[1,3], and Johannes Bieser[1]

[1]Matter Transport and Ecosystem Dynamics, Helmhotz-Zentrum Hereon, Geesthacht, Germany
[2]Benthic Ecology, Alfred Wegener Institute, Am Alten Hafen 26, 27568 Bremerhaven, Germany
[3]Universität Hamburg, Institute for Marine Sciences, Mittelweg 177, 20146 Hamburg, Germany

Correspondence: David J. Amptmeijer (davidamptmeijer@gmail.com)

Abstract. Methylmercury (MeHg) is a bioaccumulative neurotoxin that poses a risk to human health through seafood consumption. Sponges play a complex role in mercury (Hg) cycling, with measurements showing an unusually high inorganic Hg (iHg) content in Low Microbial Assemblage (LMA) sponges and an even higher iHg content in High Microbial Assemblage (HMA) sponges. At the same time, the MeHg content remains low, particularly in HMA sponges. In this study, we used a 1D water column model to investigate the bioaccumulation of MeHg in sponges. It has been hypothesized that this low MeHg content is due to active demethylation in HMA sponges. Our model results suggest that the consumption of dissolved organic matter (DOM) in LMA sponges can explain the low observed MeHg content, and higher DOM consumption in HMA sponges can account for the even lower MeHg content in HMA sponges. If demethylation occurs, a low demethylation rate of 1% per day can account for the observed difference between LMA and HMA sponges. Although DOM consumption increases iHg bioaccumulation in both LMA and HMA sponges, it does not explain the extremely high values observed, suggesting a reduced iHg release rate in sponges. We propose that this low Hg release rate is due to sulfated polysaccharides, which are abundant in sponges, especially HMA sponges. Finally, our model suggests that HMA sponges could potentially reduce the MeHg content in benthic fish by up to 45% when HMA sponges dominate at the base of the food web. While these findings suggest an important role of sponges in Hg cycling and emphasize the need to preserve sponge grounds to mitigate human MeHg exposure through seafood, this should be seen as a hypothesis-generating model result which would require further empirical validation.

1 Introduction

Mercury (Hg) and methylmercury (MeHg) are both toxic pollutants that can bioaccumulate throughout the food chain (Mason et al., 1995). Although both Hg and MeHg can bioaccumulate, MeHg has a much higher bioaccumulation potential and greater toxicity (Jeong et al., 2024). MeHg bioaccumulates especially in high-trophic-level fish, which pose health risks to humans when consumed. In commercially important species such as Mediterranean bluefin tuna (*Thunnus thynnus*), Hg concentrations can increase by up to 8 orders of magnitude compared to seawater levels (Storelli et al., 2002; Tseng et al., 2021). Consumption of MeHg-polluted fish causes adverse health effects in humans and is estimated to cost the European Union up to 8-9 billion per

https://doi.org/10.5194/egusphere-2025-5377
Preprint. Discussion started: 12 November 2025

annum, mostly due to the loss of intelligence in children (Bellanger et al., 2013). Furthermore, Hg pollution leads to reduced fish stocks and restrictions on fishing practices, which can decrease supply and profitability in the fishing sector (Pacyna et al., 2006). Hg is present in the marine ecosystem in several distinct chemical species that form a dynamic equilibrium. A table with used abbreviations in this study including the different Hg species is shown in Table 1. Important species for marine Hg cycling are elemental Hg (Hg^0), dissolved Hg (Hg^{2+}), monomethyl mercury ($MMHg^+$), dimethylmercury (DMHg), and cinnabar (HgS). Hg0 and DMHg are both dissolved gaseous Hg that can evaporate from the surface ocean. Hg^{2+} and $MMHg^+$ are the only Hg species known to bioaccumulate (Morel et al., 1998). HgS can be precipitated and is considered the most important sink of Hg out of the biosphere. In this paper, the sum of all Hg species is referred to as Hg, the sum of both $MMHg^+$ and DMHg is referred to as MeHg, and all non-methylated Hg is referred to as inorganic Hg (iHg). As only $MMHg^+$ and Hg^{2+} have been shown to bioaccumulate, we will model the bioaccumulation of these two Hg species.

The primary pathway for MeHg bioaccumulation in aquatic ecosystems begins with direct uptake of MeHg from the water column by respiration, absorption, or swallowing. When this uptake results in higher concentrations within the organism than in the surrounding water, it is called bioconcentration. This occurs because MeHg binds strongly to organic material, especially thiol (-SH) groups, which are common in proteins (**?**). This process can increase MeHg concentrations within organisms by up to 100,000 times compared to concentrations in surrounding water (Lee and Fisher, 2016). This process is dependent on the surface area of organic membranes with water, and is therefore efficient in small animals; because of this, bioconcentration is especially important at the base of the food web, in organisms such as phytoplankton (Mason et al., 1995). When predators consume phytoplankton, these predators can take up MeHg that is bioconcentrated in phytoplankton very efficiently, leading to a higher concentration of MeHg in predators compared to their prey (Mason et al., 1996). This process of increasing MeHg with increasing trophic positions is called biomagnification and can lead to extremely high concentrations of MeHg in high trophic level animals, including species that are often consumed by humans (Lavoie et al., 2013).

1.1 The role of DOM in MeHg bioaccumulation

Dissolved Organic Matter (DOM) plays a crucial role in the bioaccumulation process. DOM can bind to MeHg and these DOM-MeHg complexes can be transported to phytoplankton through transport channels (Garcia-Arevalo et al., 2024). The bioavailability of MeHg is influenced by the characteristics of DOM, particularly the presence of specific functional groups within the DOM, notably thiols (Seelen et al., 2023).

Although phytoplankton forms the base of most marine food webs, not all trophic chains start with living phytoplankton. While most aquatic animals can only feed on material that is large enough to be filtered from the water, sponges, in particular, can consume DOM (De Goeij et al., 2013). Due to their pumping activity, sponges and their associated microbes can process and filter up to 24,000 liters of seawater per day (Vogel, 1974). Sponges can utilize symbiotic bacteria, but there is a strong distinction between High-Microbial-Assemblage (HMA) sponges and Low-Microbial-Assemblage (LMA) sponges. HMA sponges can have 10^8 to 10^{10} bacteria g^{-1} sponge, whereas LMA sponges have 10^5 to 10^6 bacteria g^{-1} sponge, which is roughly equivalent to the concentration of bacteria in seawater (Hentschel et al., 2012). Symbiotic bacteria can extract DOM out of the water for consumption, giving sponges the rare ability among marine animals to utilize DOM as a food source.

https://doi.org/10.5194/egusphere-2025-5377
Preprint. Discussion started: 12 November 2025

This difference in the size of the microbiome also means that HMA sponges have a higher assimilation efficiency of DOM compared to LMA sponges (Bart et al., 2020). LMA sponges, on the other hand, compensate for the decreased size of their microbiome and their ability to utilize DOM as a food source by relying on pumping large water concentrations and filtering more particulate organic material (Hentschel et al., 2006). While in HMA sponges, the high abundance of associated microbes can account for **up to 35% to 40%** of the total biomass (Vacelet and Donadey, 1977). This high microbial biomass is crucial for the sponge's nutrition and overall health, as these microbes play essential roles in nutrient cycling and processing DOM within the sponge. Furthermore, bacterial symbionts from HMA sponges possess a wide variety of genes that confer unique biogeochemical attributes not commonly found in other animals (Webster and Thomas, 2016). The unique ability of sponges to consume DOM can have a ripple effect throughout the food chain since HMA sponges utilize organic matter that is not available to other organisms and transfer it to higher trophic levels (Hanz et al., 2022). In this way, they play an important ecological role as pseudoautotrophic producers and facilitate the indirect transfer of DOM via sponges to higher trophic level predators, such as fish, starfish, or sea urchins, which feed on sponges. Additionally, DOM assimilated into larger organic material by sponges can be excreted as detritus, which can be consumed by other animals in a process known as the sponge loop (De Goeij et al., 2013).

1.2 Hg in sponges

Studies analyzing iHg and MeHg in sponges found extreme variability in the iHg and MeHg content. Orani et al. (2020) found that in the Mediterranean Sea sponges generally have extremely low MeHg and a low MeHg/Hg ratio of 4%, while sponges in the intertidal area of the Celtic Sea have very high MeHg concentrations and high MeHg / Hg ratios of between 7 and 28%. Recent efforts in sponge identification suggest that of the 4 sponges sampled from Orani et al. (2020) from the Mediterranean Sea, 3 species are classified as LMA sponges; *Acanthella acuta* (Gloeckner et al., 2014), *Cymbaxinella damicornis*, recently reclassified under the genus *Axinella* (Erwin et al., 2015), and *Haliclona fulva* (García-Bonilla et al., 2019), while 1 sponge, *Chondrilla nucula*, is classified as HMA (Thiel et al., 2007). Remarkably, all sampled sponges have an extremely low MeHg concentration and a low MeHg/Hg ratio, but the HMA sponges have both lower MeHg and higher iHg compared to the sampled LMA sponges.

The low MeHg content in sponges in the Mediterranean Sea is proposed to be caused by active *in vivo* MeHg demethylation by Orani et al. (2020). This is because HMA sponges have been found to contain bacterial symbionts that possess the MerA and MerB genes (Santos-Gandelman et al., 2014). The MerA gene transcribes the mercuric reductase protein that converts Hg^{2+} to volatile Hg^0 and merB transcribes for organomercurial lyase, which catalyzes the breakdown of C-Hg bond through protonolyses and can demethylate toxic MeHg into less toxic Hg^{2+} (Mathema et al., 2011), but this does not explain the low concentration of MeHg in LMA sponges. An alternative proposal for the low MeHg concentration of HMA sponges is that this is low due to the consumption of DOM. This is proposed in (Amptmeijer et al., 2025b), which is a modeling study in which the effect of the feeding strategy of iHg and MeHg is modeled. In this model, the feeding strategy was isolated and this model does not consider other biological factors that might impact bioaccumulation, such as *in vivo* demethylation, the extended lifespan of sponges, and their low metabolic rate. Additionally, the model is simulated in conditions representing the North Sea, where

https://doi.org/10.5194/egusphere-2025-5377
Preprint. Discussion started: 12 November 2025

HMA sponges are not abundant. The model presented in this manuscript expands on the model presented by Amptmeijer et al. (2025b) by creating a more realistic model of sponges. We focus on incorporating the life cycles and feeding behaviors of megabenthos groups to enhance the understanding of iHg and MeHg bioaccumulation in Mediterranean Sea sponges, while running the simulation under hydrodynamic and climatological conditions typical of the Western Mediterranean Sea, where HMA sponges are common.

1.3 The hypotheses

We test the following hypotheses using a modeling approach:

- The low MeHg concentrations in LMA sponges can be attributed to their consumption of DOM, while the even lower levels observed in HMA sponges are likely due to both DOM consumption and active demethylation.
- The elevated iHg concentrations in both LMA and HMA sponges can be explained by their uptake of iHg from DOM.
- Sponges can reduce the MeHg concentration in benthic fish by having a low MeHg concentration and forming the base of the food web

To test these hypotheses, we constructed a model to trace the bioaccumulation of MeHg within the Mediterranean Sea food web in the Bay of Villefranche, a region of notable concern with respect to Hg contamination (Claisse, 1989). This enables us to initially assess the levels of iHg and MeHg accumulating in LMA sponges and determine if our model can accurately replicate the observed data. The demethylation rate necessary to account for the observed differences between LMA and HMA sponges was afterwards estimated. Finally, the model was used to assess the differences in MeHg bioaccumulation in fish in a setup with and without sponges to see if sponges influence the MeHg bioaccumulation in fish. Given the limited observational data available and that the model is 1D without a vertical component, this study serves as a proof-of-concept to evaluate whether these mechanisms are numerically plausible, but their verification and quantification requires empirical validation.

2 Materials and methods

2.1 The model domain; The Bay of Villefranche

The Bay of Villefranche is a natural bay located just west of the French-Italian border, near the French town of Villefranche-sur-Mer. The Bay is known for its deep oligotrophic waters with steep underwater topography, rocky inlets, and sandy bottoms. The nearby Villefranche Canyon creates diverse habitats that support different benthic communities. Monitoring programs within the Bay were mainly focused on planktonic research of coastal waters (Dolan, 2014). This is the reason why similar and abundantly available long-term benthic community data from nearby areas of the Gulf of Lyon were used to evaluate our model.

https://doi.org/10.5194/egusphere-2025-5377
Preprint. Discussion started: 12 November 2025

Table 1. Definitions of Hg abbreviations.

Abbreviation	Meaning
Hg	Refers to Hg in general
Hg^{2+}	Dissolved Hg (Bioaccumulates)
Hg^{0}	Elemental Hg (Volatile)
$MMHg^{+}$	Monomethylmercury (Bioaccumulates, extremely toxic)
DMHg	Dimethylmercury (Volatile, extremely toxic)
MeHg	$MMHg^{+}$ + DMHg
iHg	Sum of all Hg that is not MeHg
DGM	Dissolved Hg^{0} and DMHg
HMA sponge	High microbial assemblage sponge
LMA sponge	Low microbial assemblage sponge
DOM	Dissolved organic matter
lDOM	Labile dissolved organic matter
sDOM	Semi-labile dissolved organic matter
rDOM	Refractory dissolved organic matter
SPs	sulfated polysaccharides

2.2 The hydrodynamic model; GOTM

The one-dimensional (1D) Generalized Ocean Turbulence Model (GOTM) is used as the hydrodynamic model, which calculates the turbulence of a vertical 1D water column setup by computing the solutions to the 1D version of the transport equation of momentum, salinity, and temperature (Bolding et al., 2021). The model is nudged to observational data sets for temperature and salinity. The setups are designed using the hGOTM tool, which is driven by gridded bathymetry data for water depth (1/240°) (GEBCO Bathymetric Compilation Group, 2020), the ECMWF ERA5 dataset for meteorological data (Wouters et al., 2021), and the World Ocean Atlas for salinity and temperature profiles (Garcia H.E. et al., 2019);

2.3 Coupling GOTM to the biogeochemical models using FABM

The MERCY v2.0 model and the ECOSMO E2E model are coupled to the GOTM model using the Framework for Aquatic Biogeochemical Modeling (FABM) (Bruggeman and Bolding, 2014). The biogeochemical models are coded into FABM. The FABM interfaces communicate the state variables between the GOTM model and the biogeochemical models. Physics is modeled with a vertical grid resolution of 0.71 grid cell m^{-1}. The model's state variables are updated every 120 seconds using the forward Euler method to solve the ordinary differential equation.

https://doi.org/10.5194/egusphere-2025-5377
Preprint. Discussion started: 12 November 2025

2.3.1 Hg cycling and speciation; the MERCY v2.0 model

Hg speciation and cycling are modeled using the MERCY v2.0 model (Bieser et al., 2023). The MERCY v2.0 model is an Hg cycling and speciation model that simulates the cycling and speciation of Hg, Hg^0, $MMHg^+$, DMHg, and HgS, its partition to detritus and DOM, and the bioaccumulation of $MMHg^+$ and Hg^{2+} while taking into account biomagnification and bioconcentration at every trophic level.

2.3.2 Carbon cycling and ecosystem dynamics; the ECOSMO E2E model

The ecosystem in which Hg bioaccumulates is simulated using an altered version of the ECOSMO E2E model. The original ECOSMO model presented by Daewel and Schrum (2013) is expanded in the ECOSMO E2E model to incorporate higher trophic levels while preserving consistency in lower trophic levels (Daewel et al., 2019). Several adjustments to this model are presented in Amptmeijer et al. (2025a) to make sure that the model, which is originally developed for carbon cycling, is also suitable for bioaccumulation. In this paper, the ECOSMO E2E model is further altered by expanding the megabenthos by splitting it into 6 megabenthos groups separated by their feeding strategies. For every group, a model organism is selected based on which group is parameterized. The megabenthos groups and model organisms are filter feeders (mussel; *Mytilus sp*), deposit feeders (lugworm; *Arenicula marina*), generalist feeders (brown shrimp; *Crangon crangon*), LMA sponges; (*Mycale hentscheli*), suspension feeders with HMA sponges (*Chondrilla nucula*), benthic predators (shore crab; *Carcinus maenas*), and benthic fish (European plaice; *Pleuronectes platessa*). The benthic fish replaces the pelagic fish that was present in the previous version of the ECOSMO model, to better represent the characteristics of the shallow water in the Bay of Villefranche. The specific species used for this model are not always the main species in these ecosystems since biological rate measurements are not available for most species. However, we assume that biological rates are representative of broader functional groups and still represent the expected ecosystem functioning.

2.4 Nutrient fluxes in the 1D model

Nutrient cycling is normally dependent on lateral fluxes that are not present in a 1D water column model. To compensate for this, an atmospheric deposition of 0.13 NO_3 μmol per day (d^{-1}), 0.13 NH_4 μmol d^{-1}, $3.93*10^{-4}$ PO_4 μmol d^{-1}, and $6.28*10^{-2}$ SiO_4 μmol d^{-1} is introduced to compensate for the burial of organic material. This approach of using atmospheric deposition as a tuning parameter follows the methodology applied in the 1D GOTM-ECOSMO-MERCY setups for the North and Baltic Seas used in Amptmeijer et al. (2025a). The deposition values are chosen to produce realistic wintertime nutrient concentrations and support chlorophyll levels in line with observed data. This is further evaluated in the model evaluation section.

2.5 The megabenthos model

The physiological parameters of megabenthos within our model are derived from rates observed in laboratory conditions or through field studies. Given the inherent variability present in biological data, definitive rates are not always available and have been inferred from the referenced studies. The deposit feeders, generalist feeders, benthic predators, and benthic fish all

https://doi.org/10.5194/egusphere-2025-5377
Preprint. Discussion started: 12 November 2025

feed based on a feeding rate and half saturation. Feeding and respiration rates are presented here as daily rates. Therefore, a feeding or respiration rate of 0.1 d^{-1} would mean that the animal consumes or respires 10% of its body weight per day. This modeling approach is based on the macrobenthos functional group in the original ECOSMO E2E model (Daewel et al., 2019). The feeding of filter feeders and HMA and LMA sponges is based on their filtration rate within the bottom grid cells of the model. These groups consume a fraction of all food in the bottom grid cell, calculated as their filtration rate [m^3 d^{-1}] divided by the volume of the bottom grid cell [m^3], giving us the uptake [d^{-1}]. There is a maximum consumption rate beyond which a higher concentration of food in the water column will not lead to a higher intake rate. It should be noted that while we estimate the feeding, respiration, and mortality rates of megabenthos based on empirical studies, the modeled animal still represents functional groups.

The uptake rates of the **deposit feeder** are taken from ex-situ studies performed on a sand-eating lugworm (*Arenicula marina*), whereas this also represents other deposit feeders such as deposit feeding gastropods in the model. The respiration rate based on this study is 0.013 d^{-1}, and the mortality rate is 0.0005 d^{-1}. The respiration rate is estimated based on the measured oxygen consumption and converted to carbon respiration, assuming a respiratory quotient of 0.85 (Rodil et al., 2019). The mortality rate is based on the observed life expectancy of 5 years. The grazing rate is 0.12, based on the measured maximum carbon consumption rate (Rijsgard and Banta, 1998; Rodil et al., 2019).

The **filter feeders** in our model are modeled after mussels (*Mytilus sp.*). They are parameterized to have a filtration rate of $9.60*10^{-4}$ m^3 d^{-1}, a maximum feeding rate of 0.21 d^{-1}, a respiration rate of 0.00867 d^{-1}, and a mortality rate of 0.0063 d^{-1} (Koopmans and Wijffels, 2008). The high filtration rate means that filter feeders can grow the fastest of all megabenthos groups in our model when food is abundant, but their high respiration rate means that they are competitively disadvantageous when food is limited.

The model organism for the **generalist feeder** is the brown shrimp (*Crangon crangon*). They eat microzooplankton, mesozooplankton, detritus, and sediment organic carbon. They are estimated to have a lifespan of 3 years, or a mortality rate of 0.0083 d^{-1}, and a maximum feeding rate of 0.12 d^{-1} (Perger and Temming, 2012). Regnault (1981) found a respiration rate of per 51μl O_2 h^{-1} in a 91 mg^{-1} d.w. shrimp, or 0.55 mg O_2 g^{-1} d.w. This can be translated into a respiration rate of 0.00752 d^{-1} based on a respiratory quotient of 0.85 (Rodil et al., 2019). As a generalist, they thrive in highly variable circumstances where their ability to use different food sources gives them a competitive advantage.

Benthic predator

The benthic predator is the mid-level trophic animal that couples Hg bioaccumulation from the base of the food web to higher trophic levels. As such, this is arguably the functional group that represents the largest number of species in our model. Rates are estimated after the shore crab (*Carcinus maenas*), but the functional group of benthic predators would also include other animals. This is because there is not one animal that feeds on all the included megabenthos groups. Notable predators of HMA sponges are, for example, white seabream (*Diplodus sargus*), the nudibranch *Hypselodoris cantabrica*, and the purple sea urchin (*Paracentrotus lividus*) (Bertolino et al., 2024; da Cruz et al., 2012; Maldonado and Uriz, 1998). The benthic predator is modeled based on laboratory studies of Wallace (1973). They found a feeding rate of 0.065 d^{-1} at 10 °C and 0.13 d^{-1} at 24

https://doi.org/10.5194/egusphere-2025-5377
Preprint. Discussion started: 12 November 2025

°C and observed that the investigated shore crabs were not active below 5 °C. In addition, they found respiration rates between 0.0277 and 0.133 d^{-1}. Based on this, we assume that benthic predators below 5 °C do not hunt; above 24 °C they have their optimum grazing rate of 0.13 d^{-1}. We used this information to approximate the temperature-dependent respiration ($R_{BP}(T)$) and grazing ($P_{BP}(T)$) rates for the benthic predator as follows:

$$R_{BP}(T) = \begin{cases} 0.00277 & \text{if } T \leq 5 \\ 0.00055 \cdot T & \text{if } 5 < T \leq 24 \\ 0.0133 & \text{if } T > 24 \end{cases}$$

$$P_{BP}(T) = \begin{cases} 0 & \text{if } T \leq 5 \\ 0.0054 \cdot T & \text{if } 5 < T \leq 24 \\ 0.13 & \text{if } T > 24 \end{cases}$$

Where T is the temperature in °C. For this benthic predator, we assume a life expectancy of 3 years or a mortality rate of 0.008 d^{-1}.

Benthic fish

The benthic fish is modeled after common species such as the common sole (*Solea solea*), gilthead seabream (*Sparus aurata*), and European flounder (*Platichthys flesus*) which are often found near the seabed among vegetation or sandy substrates. They have a strong temperature-dependent grazing rate and respiration rate. Based on the work by Fonds et al. (1992) on European plaice (*Pleuronectes platessa*) we approximate the temperature-dependent respiration ($R_{BF}(T)$) and grazing ($P_{BF}(T)$) for the benthic fish as follows:

$$R_{BF}(T) = \begin{cases} 0.005 & \text{if } T \leq 2 \\ 0.005 + 0.002 \cdot (T-2) & \text{if } 2 < T \leq 18 \\ 0.037 & \text{if } T > 18 \end{cases}$$

Max feeding rate

$$P_{BF}(T) = \begin{cases} 0.0135 & \text{if } T \leq 2 \\ 0.0135 + 0.008 \cdot (T-2) & \text{if } 2 < T \leq 19 \\ 0.129 & \text{if } T > 18 \end{cases}$$

We assume a lifespan of 5 years, which results in a mortality rate of 0.0048 d^{-1}.

A schematic overview of all functional groups of megabenthos and how they are incorporated into the ECOSMO E2E model is shown in Fig. 1.

https://doi.org/10.5194/egusphere-2025-5377
Preprint. Discussion started: 12 November 2025

2.6 semi-labile DOM

ECOSMO E2E has two forms of pelagic aquatic organic carbon, detritus, and labile DOM (lDOM) (Daewel et al., 2019). Since DOM is a key driver in giving sponges their competitive advantage over other suspension feeders, we also added semi-labile

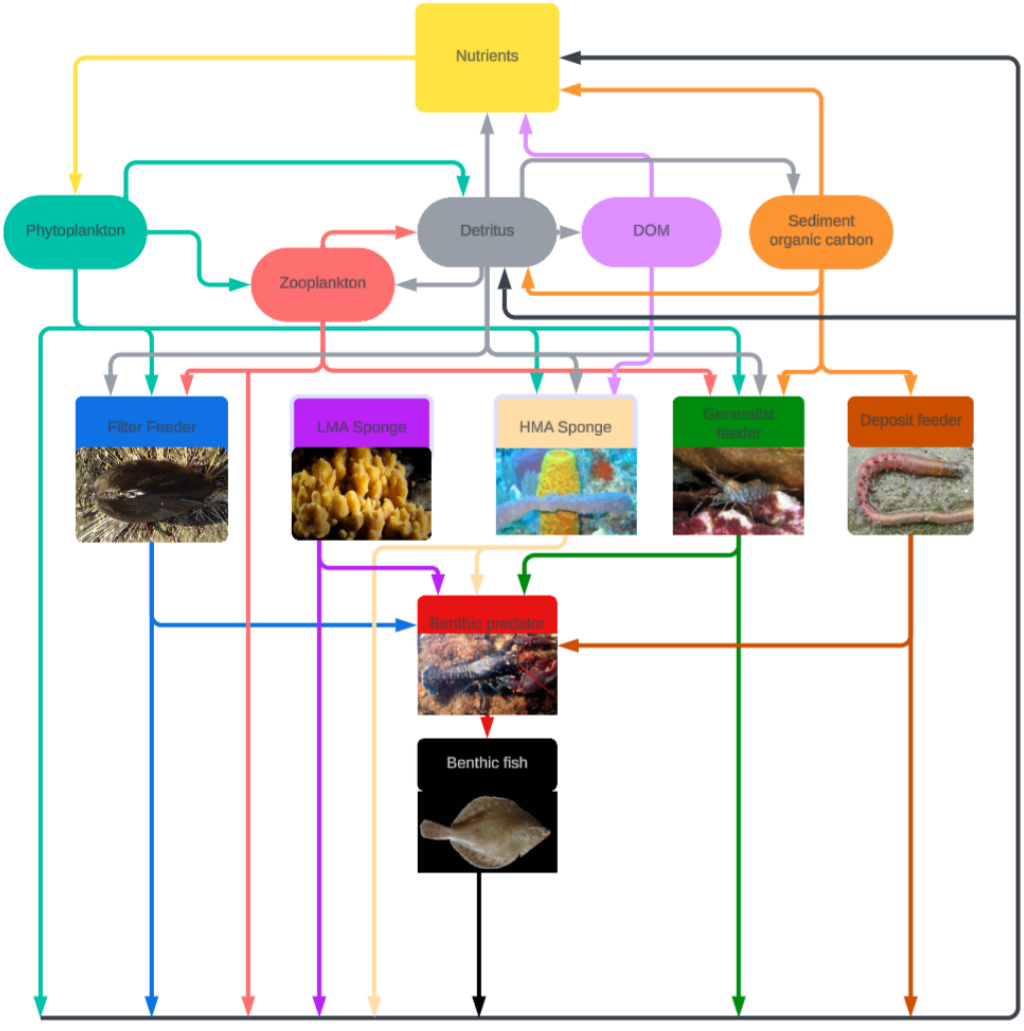

Figure 1. Schematic overview of the implemented megabenthos model. filter feeder: *Mytilus edulis* (photo by Brocken Inaglory, CC BY-SA 3.0, via Wikipedia), HMA sponge: *Aplysina fistularis* (photo by Twilight Zone Expedition Team 2007, NOAA-OE, CC BY 2.0, via Flickr), generalist feeder: *Crangon crangon* (photo by Etrusko25, Public Domain, via Wikipedia), deposit feeder: *Arenicola marina* (photo by Auguste Le Roux, CC BY 3.0, via Wikipedia), benthic predator: *Homarus gammarus* (photo by Bart Braun, Public Domain, via Wikipedia), and benthic fish: *Pleuronectes platessa* (photo by Hans Hillewaert, CC BY-SA 4.0, via Wikipedia). The photo of the LMA sponge was taken by Dr. Eric Wurtz and shared for use in this publication.

https://doi.org/10.5194/egusphere-2025-5377
Preprint. Discussion started: 12 November 2025

DOM (sDOM). Modeled sDOM does not have a sinking speed; both HMA and LMA sponges can consume it with the same efficiency as lDOM, and bacteria degrade it at the same rate as detritus. When organic material is formed in the model, it is formed as 40% lDOM, 12% sDOM, and 48% detritus. There is an additional rate of sDOM formation from detritus of 0.001 d^{-1}. These formation ratios and rates are chosen to have a realistic sDOM value of 0-50 mgC m^{-3}, based on (Lønborg et al., 2024), rather than on established rates of sDOM formation. This is described in more detail in (Amptmeijer et al., 2025b).

2.7 Refractory DOM

In addition to the sDOM added to the model, we also added refractory DOM (rDOM). This DOM is estimated to represent 97% of the global DOM pool (Baltar et al., 2021; Lønborg et al., 2024). Estimates of rDOM in the Bay of Villefranche are not available, but measurements from a bay on Medes Island estimate the concentration of total DOM at 2.56 gC m^{-3} (Ribes et al., 1999). Since our model has 0-50 mgC m^{-3} sDOM we estimate that an additional 2.5 gC rDOM gC m^{-3} could be present in our modeled domain. Given the uncertainty surrounding the extent to which sponges utilize rDOM when lDOM, sDOM, and detritus are available, and the substantial uncertainty of rDOM's binding to Hg compared to sDOM and lDOM, we run the model simulations both with and without 2.5 gC rDOM m^{-3}. When rDOM is added, it is implemented as a fixed background concentration that is not consumed by bacteria or catabolized into nutrients. This rDOM reacts within the model in two ways. First, HMA sponges can take up rDOM. Since rDOM is represented as constant background concentrations, it is unaffected by sponge uptake. To address this, and considering its low energy value as a food source for sponges, its uptake is limited to 10% efficiency compared to fresh DOM. Therefore, for HMA sponges, 2.5 gC rDOM m^{-3} corresponds to an equivalent of 0.25 gC m^{-3} lDOM, sDOM, or detritus in terms of its food availability. The difference in efficiency between the consumption of rDOM and other food sources is not based on a known value, but it is a necessary estimation, since if HMA sponges could feed on rDOM as efficiently as on other food fractions, they would overgrow everything, which is not what is observed in the Mediterranean Sea benthic food web. Because of this, it is used as a tuning parameter to increase the sponge biomass in a somewhat natural way, so we can evaluate the importance of the HMA sponges under different possible circumstances, and can evaluate the influence of sponges on fish MeHg bioaccumulation under a scenario with a high sponge biomass. rDOM is assumed to be mostly organic carbon with no other nutrients. The original ECOSMO E2E model assumes a Redfield Ratio in all consumers, but we deviate from this when HMA sponges consume rDOM to account for the low C:N and C:P ratio in rDOM. When HMA consumes rDOM, the biomass originating from rDOM is tracked, and when they release carbon due to respiration or mortality, the consumed rDOM is not released as labile nutrients for phytoplankton. The same is true when predators and top predators consume HMA sponges directly or indirectly. It is traced how much of the organic carbon originates from rDOM, and when this rDOM-originating organic carbon is released, it is not transferred to dissolved nutrients that are usable by phytoplankton. It is possible that in real life sponges consume rDOM that contains micronutrients, and these nutrients later may be bioavailable, but this is understudied and out of the scope of this model. To summarize, the rDOM approach offers an approximation that allows HMA sponges and their predators to achieve greater biomass without violating the mass conservation principles of the rest of the model, and rDOM does not react directly with any biota, except HMA sponges in the model.

https://doi.org/10.5194/egusphere-2025-5377
Preprint. Discussion started: 12 November 2025

The second way in which rDOM interacts in our model is through partitioning to iHg and MeHg. In the MERCY v2.0 model, the binding partitioning between lDOM and iHg and MeHg is assumed to be based on partitioning coefficient for organic material (the K_d). We use the same partitioning coefficient for lDOM, sDOM, and rDOM. A partitioning coefficient of $\log(K_d)=6.4$ for iHg and a coefficient of $\log(K_d)=5.9$ for MeHg is used. This value is the same as is used in Bieser et al. (2023) and is based on Tesán Onrubia et al. (2020).

Our rDOM implementation addresses its absence in the previous version of the ECOSMO E2E model since it is essential for understanding sponge dynamics. The constant concentration reflects rDOM's refractory nature, and the 10% efficiency assumes lower accessibility compared to fresh organic matter. This enables exploration of an under-studied mechanism in Hg cycling. We acknowledge that the rDOM implementation represents a simplified model designed to test whether this mechanism could explain observed patterns or to determine that this is numerically unlikely. The constant concentration and 10% efficiency assumptions, while necessary for model stability, require empirical validation. This means that this approach can assist our hypothesis-generating model but is not able to generate definitive answers about the importance of rDOM for either sponges or Hg cycling.

2.8 LMA and HMA sponges

LMA and HMA sponges were modeled separately. It must be stated that sponges are an incredibly diverse group, and comprehensive studies analyzing rates in sponges are rare. Because of this, we take the published rates of sponges and evaluate them as well as possible. LMA sponges have a maximum consumption rate of 0.01 d^{-1}, a filtration rate of $4.8 \cdot 10^{-4}$ m^{-3} d^{-1}, and a combined respiration and mortality rate of 0.00257 d^{-1}, based on the LMA sponge *Halichondria panicea* (Thomassen and Riisgadrd, 1995). LMA sponges feed on phytoplankton, detritus, lDOM, and sDOM.

To distinguish the LMA and HMA sponges, we make two adjustments. First, the microbiome of HMA sponges gives them the ability to consume rDOM. However, this comes at a cost. HMA sponges are denser and filter water 52%-94% slower, due to their investment in maintaining bacterial symbionts (Weisz et al., 2008). However, their uptake efficiency is higher because of the uptake of additional DOM through their symbionts. Because of this, we give HMA sponges a filtration rate of $3.60 \cdot 10^{-4}$ m^{-3} d^{-1}, which is 25% lower than the LMA sponges. In our model, HMA sponges feed on detritus, lDOM, sDOM, and rDOM. When sponges are compared to observations we assume a carbon to dry weight ratio of 1:5, based on Bart et al. (2021). It is worth mentioning that while the 1:5 ratio was measured in Atlantic Deep Sea sponges rather than Mediterranean Sea sponges, it originates from the demosponges *Geodia atlantica* which should resemble the demosponges sampled in Orani et al. (2020).

2.9 Bioaccumulation of Hg and MeHg

The parameters and interactions with respect to bioaccumulation are based on the 1D model presented in (Amptmeijer et al., 2025b). Importantly, our model models both the biomagnification and bioconcentration of both iHg and MeHg at every trophic level. In (Amptmeijer et al., 2025b) it is shown that this model can accurately model MeHg bioaccumulation at the base of the food web without tuning. The bioconcentration in phytoplankton depends on the size-dependent bioaccumulation and the

https://doi.org/10.5194/egusphere-2025-5377
Preprint. Discussion started: 12 November 2025

release rate for both iHg and MeHg. The bioconcentration in all megabenthos is based on the macrobenthos functional group from Amptmeijer et al. (2025a) and they have an uptake rate of $1.68 \cdot 10^{-5}$ m^3 mgC^{-1} d^{-1} and $2.22 \cdot 10^{-5}$ m^3 mgC^{-1} d^{-1} for iHg and MeHg, respectively. All megabenthos have a release rate of 0.04 d^{-1} for iHg while there is no additional release rate for MeHg. Additionally, both MeHg and iHg are released with respiration and mortality. For biomagnification, an iHg assimilation efficiency (AE) of 0.31 is used and a MeHg AE of 0.95, when biota or detritus is consumed. When sediment is consumed, the AE of iHg is 0.07 and 0.43 for MeHg, based on Dutton and Fisher (2012). When DOM is consumed, the AE is 0.95 for both iHg and MeHg. This is based on the work of Garcia-Arevalo et al. (2024) in phytoplankton, which shows that DOM can play an essential role in facilitating iHg transfer into cells. The assumption is that the DOM molecules are absorbed as a whole, and therefore the iHg associated with this would have a high assimilation efficiency for both iHg and MeHg.

2.10 Scenarios

We suggest that there are 2 pathways leading to HMA sponges having a lower MeHg content than LMA sponges; the consumption of DOM and *in vivo* demethylation. To assess the relative importance of both pathways we first model the bioaccumulation in HMA sponges under base conditions, where there is no rDOM for the sponges to feed on and the sponges do not demethylate. Afterwards, we simulate sponge bioaccumulation in a scenario where 2.5 gC rDOM m^{-3} is present. This allows us to quantify the effect of rDOM consumption on the bioaccumulation of MeHg in HMA sponges. We then perform a sensitivity analysis by varying demethylation rates in HMA sponges to identify the demethylation required to explain the observed MeHg bioaccumulation in LMA and HMA sponges.

Finally, we assess MeHg bioaccumulation in benthic fish by comparing the base case to the scenarios with 2.5 gC rDOM m^{-3}. This allows us to estimate the potential impact of HMA sponges on MeHg concentrations in fish. We focus on the 2.5 gC rDOM m^{-3} scenario because it represents a high HMA sponge biomass resembling a sponge reef. The goal is to evaluate whether this effect is plausible, rather than to quantify its real-world magnitude, as the 1D water column model used here is not suitable for capturing spatial complexity.

2.11 Statistical interpretation of the results

The evaluation of MeHg bioaccumulation in LMA and HMA sponges involves assessing the Mean Percentage Bias (MPB), of which the equation is shown in Table A1. This metric was chosen because typically in assessing models the bias is used, which is the average difference between model and observations; however, we could not use this due to the uneven amount of data between the model output and observations. Therefore, we first take the mean of the model output, and then estimate the percentile bias between the modeled and observed mean. This is further supported by performing a Kolmogorov–Smirnov (KS) and Wilcoxon signed-rank (W) tests. Statistical comparisons are used exploratively to compare model scenarios. The KS test is conducted using the `ks.test()` function, and the Wilcoxon signed-rank test is performed with the `wilcox.test()` function in R (version 4.1.2, "Bird Hippie"). The evaluation considers the D-statistic, the Kolmogorov–Smirnov p-value (KS-p), and the Wilcoxon p-value (W-p). All tests are based on comparisons between the average daily model outputs from the last decade of the simulation and the observations reported by Orani et al. (2020).

https://doi.org/10.5194/egusphere-2025-5377
Preprint. Discussion started: 12 November 2025

The D-statistic measures the maximum deviation between the cumulative distributions of the model and observations, thus measuring the maximum differences in the distribution. A D value below 0.1 suggests very similar distributions, values between 0.1 and 0.5 indicate minor to moderate differences, and a D value greater than 0.5 shows a large difference. The KS-p value calculates whether a significant difference between the modeled and observed distributions exists, while the W-p value estimates the significance of the difference between their medians. P-values below 0.05 for either KS-p or W-p are considered significant.

There is a large difference in sample sizes, with 3652 model data points compared to only 4 and 6 observed data points for HMA and LMA sponges, respectively. This imbalance can influence the D, KS-p and W-p values. Therefore, the KS and W test results are interpreted to compare the setups, rather than definitive indicators of model fit or mismatch. Especially for the KS test, analyzing the distribution of 4 or 6 points should not be used to come to definitive conclusions. Despite these constraints, the D, KS-p, and W-p results still provide valuable insights into the overall agreement between modeled and observed MeHg bioaccumulation patterns in HMA and LMA sponges and can help to compare the different model scenarios.

3 Model evaluation

3.1 Evaluation of Nutrient cycling

As mentioned in the methods section, the nutrient deposition is selected to create a realistic phytoplankton community to drive our megabenthos model. In our model, the wintertime nutrient concentrations are 0.12 μmol l^{-1} NH_4^+, 5.0 μmol l^{-1} NO_3^-, 0.3 μmol l^{-1} PO_4^{3-}, and 1.6 μmol l^{-1} $Si(OH)_4$. These values are on the higher end of observations in the Western Mediterranean Sea but align with elevated nutrient concentrations found in the Gulf of Lion, where surface nitrate and phosphate concentrations reach up to 3.58 $\pm$ 1.16 μmol l^{-1} and 0.2–0.3 μmol l^{-1}, respectively . While the modeled silicate concentration is on the lower end of the observed range (1.6–5.8 μmol l^{-1}), based on the World Ocean Atlas 2018, silicate is not typically a limiting factor for phytoplankton growth in the Western Mediterranean, making this value acceptable for our modeling purposes (Belgacem et al., 2021). Based on this, we conclude that the modeled nutrient concentrations are in line with observations and can be used to simulate phytoplankton in our model.

3.2 Evaluation of primary production

We evaluate the modeled chlorophyll a concentrations against NASA MODIS-A satellite chlorophyll time series, for the same geographic location (https://oceancolor.gsfc.nasa.gov/). The observational chlorophyll time series was sourced from the COPE-POD project (REPHY, 2020). The NASA combined-satellite chlorophyll data presents monthly mean values, allowing for a comprehensive comparison. To evaluate whether the model captures the general chlorophyll a dynamics of the region, we focused on monthly means. Specifically, we averaged modeled chlorophyll values for each calendar month over the last decade of the simulation (e.g., the mean of all Januarys, all Februarys, etc.), and compared these to the corresponding monthly means from the NASA dataset.

https://doi.org/10.5194/egusphere-2025-5377
Preprint. Discussion started: 12 November 2025

While this approach smooths over interannual variability, it offers a way to assess whether the model captures the typical seasonal cycle and magnitude of phytoplankton. Given our focus on bioaccumulation processes, this comparison helps ensure that the modeled phytoplankton concentrations are within a realistic range and appropriate for driving biogeochemical dynamics in the Bay of Villefranche.

The results of the chlorophyll comparison between the model and the observations are shown in Fig. 2a, and the corresponding Taylor diagram is shown in Fig. 2b. The equations from which the metrics are derived are shown in Table A1. The modeled and observed chlorophyll concentrations exhibit a Pearson correlation of 0.59. The root mean square error (RMSE), is 0.127 mg m^{-3}. The maximum observed chlorophyll is 0.54 mg m^{-3} and modeled is 0.55 mg m^{-3}, while the observed mean is 0.31 mg m^{-3} and the modeled mean is 0.28 mg m^{-3}, resulting in a mean bias of -0.028 mg m^{-3}. Overall, the comparison reveals a low bias and relatively high correlation, indicating that the modeled phytoplankton dynamics are consistent with expectations for the Bay of Villefranche and provide a suitable basis for the biogeochemical processes explored in this study.

3.3 Evaluation of the megabenthic biomass

The benthic communities in this area have high specialization and display a patchy distribution, complicating the evaluation of our 1D model. According to Rosenberg et al. (2003), biomass values in the shallow Bay of Lyon vary widely, between 0 and 40 g ash-free dry weight m^{-2}, showing notable regional differences. Despite this, our modeled benthic biomass at 17 m ranges between 3.5 and 5 gC m^{-2}, as shown in Table 2 and visualized in Fig. 3. This means that the biomass in our model is within the observed range. In the Gulf of Lyon, distinct benthic communities dominated by filter feeders (e.g., Spisula subtruncata, Venus ovata), deposit feeders (Scoloplos armiger), and generalist predators (Nephtys hombergii) have been identified (Labrune et al., 2007; Fromentin et al., 1997; Rosenberg et al., 2003). Although our 1D model cannot resolve these complex spatial differences, our model does support stable populations of all megabenthic functional groups, making it a reasonable representation of the general benthic community structure in the area.

3.4 Evaluation of Hg and MeHg concentrations

Bioaccumulation starts with the dissolved concentration of the pollutants. Therefore, it is essential to assess that the MERCY v2.0 model generates concentrations of Hg and MeHg that are in line with observations. The modeled and observed aquatic concentrations of iHg and MeHg are shown in Table 3. Our model estimates Hg and MeHg concentrations in the Bay of Villefranche of 1.00±0.071 and 0.019±0.005 pM respectively. Observations in shallow coastal stations in the Gulf of Lion by Cossa et al. (2017) found mean Hg concentrations of 1.52±1.00 pM and MeHg concentrations of 0.026±0.024 pM, though some MeHg concentrations were below the detection limit, introducing uncertainty. This means that our modeled Hg and MeHg concentrations are well within the observed range and within 1 standard deviation, with a MPB of -34% for Hg and -26% for MeHg compared to the observed mean. Based on these results, we conclude that our model reproduces observed Hg and MeHg concentrations in the water, making it suitable to be used in our bioaccumulation modelling framework.

https://doi.org/10.5194/egusphere-2025-5377
Preprint. Discussion started: 12 November 2025

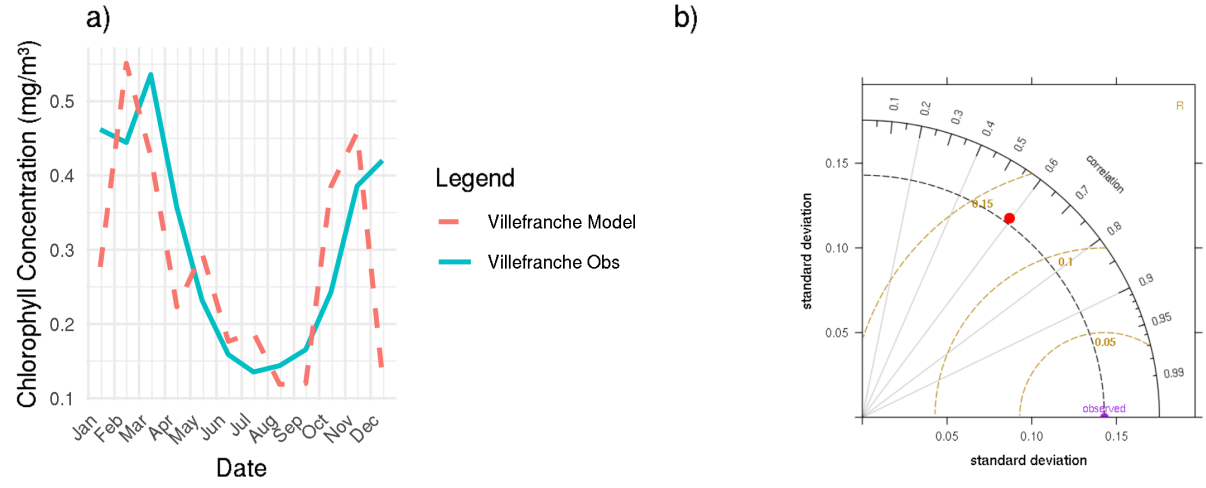

Figure 2. Validation of modeled chlorophyll concentrations. a) Monthly means over the last 10 years from the model and NASA MODIS-A satellite chlorophyll time series. b) Taylor diagram comparing the model and observations, showing a Pearson correlation coefficient of 0.59 and a root mean square error (RMSE) of 0.13 mg m^{-3}, based on monthly means of the 10-year averages.

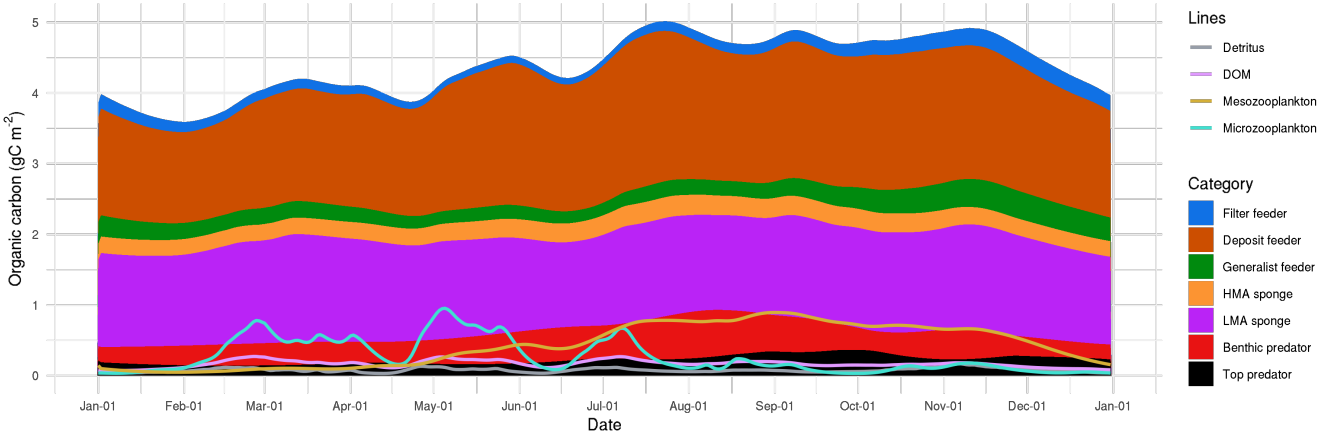

Figure 3. The 10-year average consumer biomass in the base model. Macrobenthos biomass is stacked and pelagic microzooplankton, mesozooplankton detritus and DOM is plotted as lines on top. DOM in this plot is the sum of labile and semi-labile DOM. Macrobenthos biomass is relatively consistent for all groups but dominated by deposit feeders and LMA sponges. Microzooplakton have a spring bloom whereas mesozooplankton are highest in autumn.

https://doi.org/10.5194/egusphere-2025-5377
Preprint. Discussion started: 12 November 2025

Table 2. Model results for the biomass and bioaccumulation in the Bay of Villefranche. Biomass is shown in mgC m^{-2} and bioaccumulation in ng Hg gC^{-1}, so pelagic biomass was integrated over the watercolumn depth.

Category	**Biomass**		**iHg**		**MeHg**	
Functional group	Mean	SD	Mean	SD	Mean	SD
Generalist feeders	256	177	67	8	22	5
Deposit feeders	1741	614	64	7	18	3
Filter feeders	158	118	62	9	29	9
HMA sponges	252	82	168	42	27	5
LMA sponges	1375	692	116	20	26	8
Benthic predators	382	425	61	5	36	7
Benthic fish	226	231	61	10	61	10
Microzooplankton	16	26	37	21	12	4
Mesozooplankton	25	23	55	13	12	3
Phytoplankton	41	32	1	3	2	4
Detritus	5	4	453	32	3	1
DOM	168	108	729	49	4	2

3.5 Evaluation of the MeHg bioaccumulation

The bioaccumulated iHg and MeHg per functional group are shown in Table 2. Observations distinguishing MeHg bioaccumulation in megabenthic organisms to compare our model results to are rare. We found measurements for MeHg bioaccumulation in phytoplankton, microzooplankton, and mesozooplankton by Tesán-Onrubia et al. (2023), and mesozooplankton, whereas Llull et al. (2017) reported measurements in fish. Assessing fish is challenging because our functional group encompasses several benthopelagic predators with varying MeHg levels. Thus, we present the range of observed MeHg content for the most common benthopelagic predators in the region, namely, the European hake *(Merluccius merluccius)* and the common sole *(Solea solea)*, as illustrated in Table 3. We assumed a carbon-to-weight ratio of 1:2 for fish and zooplankton based on Ricciardi and Bourget (1998), and for phytoplankton, a 1:3 ratio based on Cushing (1958). Fish bioaccumulation data were reported in wet weight; we converted this to dry weight, assuming a dry weight-to-wet weight ratio of 1:5 based on Cresson et al. (2017). Since the SD was not available for the comparison to fish, we calculated the mean based on the weighted average. Although the data are insufficient for robust statistical analysis, the average MeHg content is 46 ng Hg mgC^{-1} for European hake and 69 ng Hg mgC^{-1} for common sole while the weighted average of both species together is 60 ng Hg mgC^{-1}, as recorded by Llull et al. (2017). Consequently, our model value of 61 ng Hg mgC^{-1} falls within the observed range for the benthopelagic predatory fish considered in our model.

https://doi.org/10.5194/egusphere-2025-5377
Preprint. Discussion started: 12 November 2025

Table 3. Comparison of modeled MeHg bioaccumulation against available observations. Bioaccumulation is shown in ng Hg mgC^{-1} and the concentration of aquatic Hg and MeHg in pM. The phyto-and-zooplankton data is compared to samples from Tesán Onrubia et al. (2020), while the benthic fish data is compared to samples of European hake *(Merluccius merluccius)* and common sole *(Solea solea)* presented by Llull et al. (2017). All values are reported as the mean±SD, except for the observations in fish, where the SD was not available and is instead shown as the mean (min–max) of the observations.

	Modeled MeHg	Observed MeHg
Aquatic Hg	1.00 ± 0.071	1.52 ± 1.00
Aquatic MeHg	0.019±0.005	0.026 ± 0.024
Phytoplankton	0.6±2	0.8±1
Microzooplankton	6±2	3±2
Mesozooplankton	6±2	6±3
Benthic fish	61±10	60 (33–120)

4 Results

4.1 Expected demethylation rate of HMA sponges

Figure 4 shows the bioaccumulation of MeHg in HMA sponges. Without demethylation, the average bioaccumulation of MeHg is higher than the observations in HMA sponges. Having a demethylation rate of 1% d^{-1} reduces the bioaccumulation of MeHg to 10 ng Hg gC^{-1}, which better aligns it with the average observed MeHg concentration of 13 ng Hg gC^{-1} in HMA sponges. Furthermore, increasing the demethylation rate to 2.5% per day aligns the MeHg content of the HMA sponges with the lowest observations in the HMA sponges. The statistical comparison of the base model and the scenario with 1% and 2.5% demethylation d^{-1} is shown in Table 4. In the base model, there is a positive MPB for the MeHg content of HMA sponges (+136%) and the KS-p of <0.001 and W-p of <0.001 show a significant variation between the observed and modeled data, both in their distribution and median values. In the scenario where HMA sponges have 1% demethylation, the HMA sponges have a smaller negative bias (-23%) while the D statistic of 0.45 shows a minor difference in the distribution of the modeled and observed bioaccumulation, while the KS-p of 0.39 shows that this difference is not statistically significant. Additionally, the W-p of 0.79 shows that there is also no statistically significant difference between the observed and modeled median MeHg bioaccumulation. In the 2.5% demethylation d^{-1} scenario, the KS-p and W-p values show no significant difference between this scenario and the observations, however their value of 0.0072 and 0.0019 are considerably lower compared to the 1% d^{-1} scenario. These reduced p-values, combined with the high D value of 0.84 and an increased negative MPB of 62% show that the 2.5% demethylation d^{-1} underestimates the MeHg content of HMA sponges and has lower agreement with the observations than the scenario with 1% demethylation d^{-1}. Under our parameterization assumptions, the model suggests that demethylation rates of 1% d^{-1} provide reasonable agreement with observations, though this depends critically on uncertain uptake parameters.

https://doi.org/10.5194/egusphere-2025-5377
Preprint. Discussion started: 12 November 2025

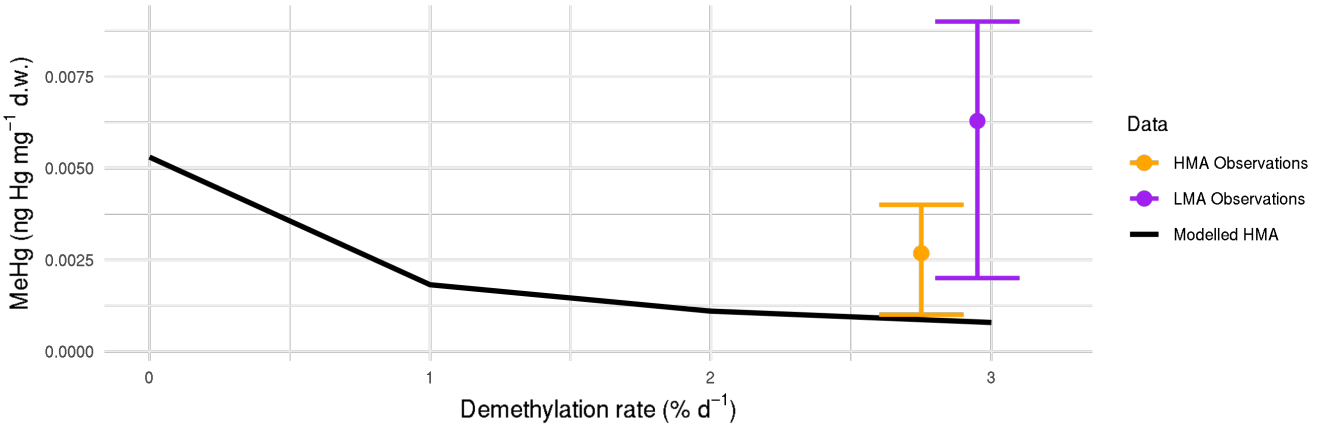

Figure 4. The modeled mean MeHg concentration in HMA sponges with different demethylation rates. Without demethylation, MeHg levels in HMA sponges align with those observed in LMA sponges, as indicated by the purple sidebar. A demethylation rate of 2.5% d^{-1} reproduces the minimum observed MeHg concentration in modeled HMA sponges, while a rate of 0.5% d^{-1} reproduces the maximum, as shown by the orange sidebar. A demethylation rate of 1% d^{-1} in HMA sponges provides the best agreement with the observed mean when rounded down to the nearest 0.5%.

4.2 Low MeHg due to DOM consumption in HMA sponges

We investigate the hypothesis that HMA sponges can have low MeHg due to their reliance on DOM as food. To investigate this we ran the model with 2.5 gC rDOM m^{-3}, which could be consumed by HMA sponges. Table 4 presents the results of MeHg bioaccumulation in LMA and HMA sponges alongside the outcomes of the KS-and-W tests, in comparison with the observations reported by Orani et al. (2020). In LMA sponges, a KS-p value of 0.32 and a D-statistic of 0.36 suggest no substantial difference in the modeled and observed distribution, while the MPB of -13% indicates a small bias between the modeled and observed mean. This is supported by a W-p of 0.23 which indicates no significant deviation between the modeled and observed median. For HMA sponges, there is no significant discrepancy between the observed and modeled distributions as signified by a KS-p value of 0.35. Additionally, the D-statistic of 0.46 indicates a moderate similarity between the modeled and observed distributions. The MBP of -23% along with a W-p value of 0.33 indicates a small bias in the mean, and no significant difference between the modeled and observed median. To summarize, in the scenario with 2.5 gC rDOM m^{-3} there is no significant difference in either the median or the distribution of MeHg bioaccumulation in both LMA and HMA sponges. Since the consumption of rDOM alone accounts for the low MeHg levels in HMA sponges, the model was not rerun with a demethylation rate and 2.5gC m^{-3}, as this was unnecessary to explain the observed low MeHg concentrations in HMA sponges.

4.3 Low MeHg bioaccumulation in fish due to rDOM consumption in HMA sponges

In our model, consumption of rDOM can influence MeHg bioaccumulation in three ways. First, in our current parameterization, rDOM binds dissolved MeHg, with the same strength as lDOM and sDOM. If we include rDOM, the MeHg concentration

https://doi.org/10.5194/egusphere-2025-5377
Preprint. Discussion started: 12 November 2025

Table 4. Observed and modeled bioaccumulation of MeHg in LMA and HMA sponges The mean, minimum, and maximum observed and modeled values are shown. Bioaccumulation values are shown in ng Hg mgC^{-1}. For the model scenarios, the mean percentile bias (MBP), the Kolmogorov–Smirnov p-values (KS-p) and D-statistic (D) are shown, as well as the Wilcoxon p-value (W-p). A * marks a significant difference at the 95% confidence level between the model and observations.

	LMA							HMA						
	Mean	MPB (%)	Min	Max	KS-p	D	W-p	Mean	MPB (%)	Min	Max	KS-p	D	W-p
Observations	31	–	10	45	–			13	–	5	20	–		
Base model	30	-3	18	72	0.12	0.45	0.26	31	+138	22	52	<0.001*	1.0	<0.001*
2.5 gC rDOM	27	-13	9	69	0.32	0.36	0.23	10	-23	3	39	0.35	0.46	0.33
1% Demethylation	29	-6	18	71	0.12	0.45	0.24	10	-23	7	30	0.39	0.45	0.79
2.5% Demethylation	25	-19	14	50	0.014	0.59	0.078	5	-62	3	16	0.0072	0.84	0.019

* indicates signicant deviations between the model and observations at the 95% confidence interval.

per DOM can be reduced due to biomass dilution. This will result in lower concentration of MeHg in suspension feeders consuming DOM, and consequently in predators consuming these suspension feeder. Secondly, the consumption of rDOM by HMA sponges allows the consumption of carbon that is otherwise not bioavailable. This increases the biomass of HMA sponges, and consequently, it increases the biomass of the benthic predator and benthic fish. The shift in biomass causes a shift in the diet of the benthic predator; in the base model, the majority of their diet would consist of deposit feeders and LMA sponges, whereas in the 2.5 gC rDOM setup, their diet would mostly consist of HMA sponges followed by deposit feeders. Since HMA sponges have an extremely low MeHg concentration, this results in low MeHg in benthic predators and, consequently, in benthic fish. The concentration of MeHg in benthic fish is 68 ng Hg g^{-1} in the base model and only 61 ng Hg g^{-1} in the setup with 2.5 gC $rDOM^{-3}$. If we run the model with 2.5 gC $rDOM^{-3}$, but without HMA sponges, the bioaccumulation of MeHg in fish is 124 ng Hg mgC^{-1}. This means that the HMA sponges in this setup reduce the MeHg content of the fish by 45%. This effect is not present in the base model, nor in the setup with 1% demethylation d^{-1}, which can be explained by the low biomass of HMA sponges in the base setup compared to the 2.5 gC rDOM m^{-1} setup. This shows that the 45% reduction is an upper bound of the reduction that can be expected in benthic fish in ecosystems that are dominated by HMA sponges at the base of the food web compared to ecosystems without sponges.

4.4 The maximum and minimum demethylation rates

Since we can replicate the low MeHg content of both LMA and HMA sponges in the 2.5 gC rDOM scenario, we conclude that *in vivo* MeHg demethylation is not necessary to explain the observed iHg and MeHg content of either LMA or HMA sponges. However, it must be noted that the bioconcentration rates of iHg and MeHg in HMA sponges in the model are very uncertain. Because of this, it is also possible that the uptake rate is higher, which would mean a higher demethylation rate is necessary to explain the observed values. The iHg concentration in LMA and HMA sponges can be assessed by simulating a tenfold rise in LMA sponge uptake rates and a twentyfold rise for HMA sponges. This results in uptake rates of $1.68 \cdot 10^{-4}$ and $3.35 \cdot 10^{-4}$ in m^3 mgC d^{-1} for iHg in LMA and HMA sponges, respectively, and uptake rates of $2.20 \cdot 10^{-4}$ and $4.41 \cdot 10^{-4}$ m^3 mgC d^{-1} for MeHg.

https://doi.org/10.5194/egusphere-2025-5377
Preprint. Discussion started: 12 November 2025

The modeled iHg and MeHg concentrations under these circumstances are shown in Table 5. Under these circumstances, a demethylation rate of 16% in HMA sponges gives the best agreement with observations, rounded to the nearest full percent point.

Table 5. Observed and modeled concentrations of iHg and MeHg in LMA and HMA sponges. The High Uptake (HU) models has uptake rates of $1.68 \cdot 10^{-4}$ and $3.35 \cdot 10^{-4}$ in m^3 mgC^{-1} d^{-1} for iHg in LMA and HMA sponges, respectively, and uptake rates of $2.20 \cdot 10^{-4}$ and $4.41 \cdot 10^{-4}$ m^3 mgC^{-1} d^{-1} for MeHg in LMA and HMA sponges respectively. In the low Release Rate (LR) model the release rate of iHg is reduced and this is equal to the respiration rate. In the LR model the earlier estimated 1% d^{-1} *in vivo* demethylation rate is used while in the HU model the *in vivo* demethylation rate required to reproduce observels MeHg levels is estimated to be 16% d^{-1}. Additonally the mean percent bias (MPB) between the modeled and observed concentration is shown. All bioaccumulation values are in ng Hg mgC^{-1}.

	iHg					MeHg				
	Observed	Model (HU)	MPB (%)	Model (LR)	MPB (%)	Observed	Model (HU)	MPB (%)	Model (LR)	MPB (%)
LMA	696	659	6	592	18	31	122	−75	28	11
HMA	1523	1476	3	1448	5	13	13	0	10	30

4.5 The high iHg of LMA and HMA sponges.

An additional method for the model to reproduce the high iHg content of sponges is to reduce the release rate. As shown in Table 5, the model also reproduces the high iHg content of both LMA and HMA if we assume that iHg is strongly retained in sponges and only released equal to the respiration rate of sponges. This model is referred to as the Low Release (LR) rate model. In this parameterization, there is no additional release rate of iHg in sponges. This parameterization can reproduce both the iHg and MeHg bioaccumulation in both LMA and HMA sponges with an MPB of 30% or lower.

5 Discussion

A summary of the results is shown in Fig. 5. Here we see that the model can produce the observed MeHg concentration in both LMA and HMA sponges if we assume either rDOM consumption or *in vivo* MeHg demethylation in HMA sponges of 1%. Additionally, it shows that if we assume a reduced release rate of sponges, the model can replicate the high iHg and low MeHg concentration in both LMA and HMA sponges. In this study, we tested several different scenarios for the bioaccumulation of iHg and MeHg in sponges; here we discuss the differences between these scenarios and how the results of this study can help us better understand the bioaccumulation of Hg in sponges.

https://doi.org/10.5194/egusphere-2025-5377
Preprint. Discussion started: 12 November 2025

5.1 With or without rDOM; what is the most realistic scenario

As mentioned in the model development segment, an rDOM concentration of 2.5 mgC m^{-3} is observed. However, as the name suggests, this rDOM is refractory and generally unresponsive. This raises the question as to what degree it should be incorporated in the model. There are 2 key questions;

- To what degree do sponges feed on rDOM compared to lDOM and sDOM
- Does Hg bind with equal preference to rDOM, sDOM and lDOM, and is this different for iHg and MeHg.

An argument for focusing solely on lDOM and sDOM is presented by Seelen et al. (2023). They show that the thiol content of DOM is lower in marine environments than in rivers and that DOM of terrestrial origin has a stronger affinity to bind MeHg as it is richer in thiol groups. If terrestrial DOM that is non-refractory has a considerably higher affinity to bind DOM, it is likely that this transfers MeHg to sponges upon consumption. If this is the case, having lDOM and sDOM in our model to bind and transfer MeHg, while excluding rDOM, might replicate real-world circumstances. Where labile fractions of DOM dominate MeHg binding and transfer.

Additionally, while it is currently understood that HMA sponges can consume DOM, including rDOM, the degree to which they do this is poorly understood. In shallow Mediterranean Sea water, other food sources are available. Because of this, HMA sponges might predominantly feed on the more labile fractions of DOM, and rDOM could play a minor or insignificant role, both in carbon cycling and in MeHg bioaccumulation.

Arguments in favor of including rDOM are that we know it is present in large concentrations and there is only limited evidence to suggest it does not play a major role in both Hg and carbon cycling. This is also supported by our model. Our

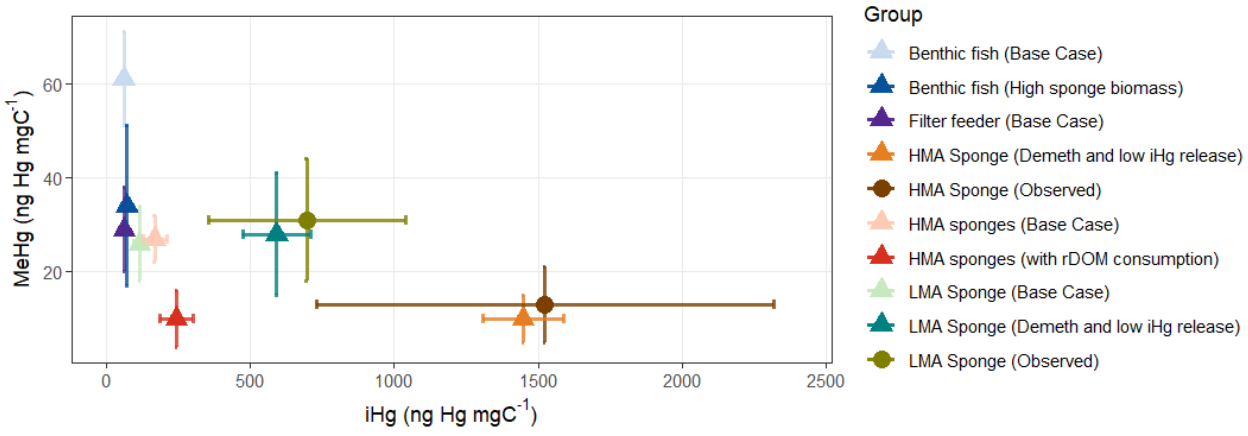

Figure 5. Summary visualising the important results. The triangles represent model values and the circles observations of LMA and HMA sponges. The scenario with a demethylation rate of 1% d^{-1} and reduced Hg release rate has a strong overlap with the observed LMA and HMA sponges. The MeHg concentration in fish (Blue) is reduced by 45% in the scenario where sponges have high biomass.

https://doi.org/10.5194/egusphere-2025-5377
Preprint. Discussion started: 12 November 2025

model shows good agreement (% MPB < 26) with no significant difference (ks-P > 0.28) between the modeled and observed MeHg concentrations in both LMA and HMA sponges when we incorporate rDOM in the model.

Additionally, it is established knowledge that DOM plays an important role in Hg bioaccumulation, as demonstrated by Schartup et al. (2015), and that different DOM fractions can affect Hg bioaccumulation in distinct ways, as shown by Seelen et al. (2023). Therefore, improving the representation of DOM and detritus cycling, particularly by including distinct fractions such as rDOM, represents a logical step forward to increase Hg cycling and bioaccumulation models, even in models that do not incorporate HMA sponges.

To improve the model in this regard, more empirical data is needed to link rDOM to concentrations and composition to bioaccumulation. Improved knowledge of which fractions of DOM are consumed by LMA and HMA sponges and to which degree, coupled with a better understanding of the MeHg binding strength of this DOM fraction, could greatly improve our understanding of what drives these low MeHg concentrations in HMA sponges.

5.2 The important role of HMA sponges in lowering MeHg content of fish

While demethylation and DOM consumption can both play a role in causing the low MeHg content of sponges, especially HMA sponges, they certainly have an extremely low MeHg content. In addition, HMA sponges can have large biomass and be the main part of low-trophic-level biomass. Our model shows that this can dramatically reduce the MeHg content of higher benthic fish; in our model, this is a reduction of 45%. This percentage is, of course, highly dependent on the MeHg concentration of sponges, the MeHg concentration of other megabenthos, and the degree to which sponges are consumed. While the role of sponges in the ecosystem is understudied, it is clear that sponges are both directly and indirectly consumed by important commercial species of fish.The 45% reduction in MeHg bioaccumulation of fish represents a potential quantification of this effect under high HMA sponge biomass scenarios, while assuming HMA sponges are a critical link in the food chain. This represents an upper bound estimate that would require validation under natural conditions.

5.3 The iHg content of sponges

The model mainly focuses on explaining the low MeHg content of the sponges and the observed difference between LMA and HMA sponges. However, investigating the unusually high iHg content of HMA sponges is an essential part of the Hg sponge biochemistry and should be taken into account. We demonstrate that we can explain both the iHg and MeHg concentrations found in HMA sponges by assuming an iHg and MeHg uptake rate of $3.88 \cdot 10^{-9}$ for iHg and $5.10 \cdot 10^{-9}$ for MeHg. The issue with this parameterization is that we can offer no explanation for the low MeHg content of LMA sponges. An additional way we can reproduce the observed iHg content of sponges is sponge retain Hg stronger than other macrobenthos. We can reproduce the high iHg content of both HMA and LMA sponges if we assume that the release rate of iHg is equal to the carbon respiration rate of the sponge, which is much lower than what has been observed for other animals such as small crustaceans and bivalves (Tsui and Wang, 2004; Pan and Wang, 2011). While this is speculative at the moment, a potential explanation can be found in the unique structure of sponges. A study on the glass sponge *Euplectella aspergillum* found that they have elevated Hg levels in the spicules. *C. nucula* is a demosponge, not a glass sponge, but it still has glass spicules. But a similar buildup of iHg in

https://doi.org/10.5194/egusphere-2025-5377
Preprint. Discussion started: 12 November 2025

structural components of the sponge might be happening in other components of the sponge. Demosponges rely on a protein called spongin and sulfated polysaccharides (SPs) to bind the sponge together. A possible explanation for the reduced release rate of iHg in sponges could be that iHg remains bound to the SPs in sponges.

We propose this for three reasons.

- SPs in *C. nucula* have a very high sulfate to sugar ratio of 1:5 (Vilanova et al., 2007).
- SPs with high sulfate content have been found to bind 50 mg of Hg g^{-1} SPs (Cruz et al., 2017).
- Sponges contain up to 3% SPs, providing abundant bindings sites for iHg (Esteves et al., 2011).

Combining these observations, we can estimate that sponges with 3% dry weight SPs would be able to bind 1500 ng Hg mg^{-1} dry weight, or 7500 ng Hg mgC^{-1} assuming a 1:5 carbon to weight dry weight ratio. This is higher than observed and shows that the SPs in *C. nucula* would be able to store the observed Hg concentrations. Note that this is a rough estimation and, for example, the iHg binding data of the SPs are based on bacterially produced linear SPs rather than branched SPs produced by demosponges. It does, however, indicate that the high SPs content of the sponge could explain its high iHg content. Given that our model predicts elevated iHg concentrations in sponges due to DOM consumption, but it cannot fully reproduce the observed iHg levels, it seems the high iHg content in sponges results from a combination of both drivers.

5.4 Low MeHg in HMA sponges; Demethylation, DOM consumption or both

Since our model can reproduce MeHg concentrations without demethylation in both HMA and LMA sponges, it shows that demethylation may not be necessary to describe the observed patterns. This does not mean that demethylation cannot play a role, but since LMA sponges do not contain large amounts of sulfate-reducing bacteria that can demethylate MeHg, a compelling argument can be made based on our model that the low MeHg concentration in LMA sponges is caused by the consumption of DOM and detritus, which make up a substantial part of their diet. The even lower MeHg content of HMA sponges can then be explained by an increased dependence on DOM by HMA sponges, *in vivo* MeHg demethylation, or a combination of both.

The expected demethylation rate is linked to the uptake rate of MeHg, which is uncertain. Because of this, we see two potential pathways that lead to the observed bioaccumulation of iHg and MeHg in LMA and HMA sponges.

The scenario with no *in vivo* MeHg demethylation, as is explored in the 2.5 gC rDOM scenario, and low *in vivo* MeHg demethylation, as is explored in the 1% demethylation scenario, can both reproduce the observed MeHg concentration in LMA and HMA sponges, but lack a full explanation for the elevated iHg concentration in sponges. Because of this, we conclude that both no or low *in vivo* MeHg demethylation in HMA sponges is possible, and we supplement this paper with a proposed explanation on why sponges could have high iHg based on their chemical composition.

An alternative explanation for the observations presented in this paper is that sponges may bioconcentrate Hg at an accelerated pace, accounting for the elevated iHg levels, coupled with a rapid demethylation rate reaching up to 16%, which

https://doi.org/10.5194/egusphere-2025-5377
Preprint. Discussion started: 12 November 2025

accounts for the low observed MeHg. The challenge with this explanation is the lack of compelling evidence for a rapid *in vivo* demethylation rate in LMA sponges; thus, this model fails to reproduce the low MeHg levels observed in LMA sponges.

Consequently, we consider it most likely that the high iHg content of sponges results from their increased exposure to a reduced release rate of iHg, possible due to iHg accumulation on SPs or spongin. The low MeHg levels in LMA sponges are attributed to the consumption of DOM, while the reduced MeHg levels in HMA sponges arise from DOM consumption, possibly accompanied by an *in vivo* demethylation rate of 1%.

5.5 Limitations of the rDOM implementation

A major simplification in our model lies in the implementation of rDOM. In our setup, rDOM serves as a proxy for organic material that can be consumed by HMA sponges but is not dissimilated by non-sponge-associated microbes on timescales relevant to our model. This approach is particularly suited to a 1D configuration, where a constant flow of rDOM can be assumed throughout the system. The current implementation was chosen to ensure consistency in nutrient availability for phytoplankton growth, to preserve mass balance across the model, and to enable HMA sponges to use rDOM for growth; as such, it serves as a useful proof of concept to explore whether rDOM could play a meaningful role in ecosystem functioning. However, this implementation is limited in scope. In a 3D model or in stratified water columns where vertical mixing is reduced, rDOM transport may significantly influence the distribution and cycling of Hg. Furthermore, potential effects of rDOM, such as its role in light attenuation, are not incorporated in the model. To fully assess the role of rDOM in both HMA sponge ecology and Hg biogeochemistry, cycling, and bioaccumulation, a more realistic representation will be necessary.

5.6 Broader limitations and future research needs

Beyond the limitations of the rDOM implementation, several major limitations affect the model. The most important is the low data availability. Our entire conclusion is based on a single study of MeHg and iHg bioaccumulation in Mediterranean Sea sponges, with very limited sample sizes (n=4 for HMA and n=6 for LMA sponges).

In addition, there is major uncertainty in model parameterization. While there is relevant uncertainty in the carbon cycling component of the model, notably in the newly introduced expanded megabenthos model, the carbon stocks appear to be in line with observations. What is more pressing is the uncertainty in Hg bioaccumulation. Hg bioconcentration rates used for sponges are not based on studies in sponges and could be notably different.

We focus on qualitative model insights rather than extensive sensitivity analyses. While all parameters carry uncertainty, our primary objective is to demonstrate that the proposed mechanisms are quantitatively plausible alternatives to the demethylation hypothesis proposed by (Orani et al., 2020). Comprehensive sensitivity analyses would confirm parameter uncertainty without providing additional mechanistic insights. Rather, we demonstrate that our base parameterization can reproduce the observed bioaccumulation of MeHg in both LMA and HMA sponges linked to the consumption of DOM and rDOM, which shows that DOM consumption by LMA sponges and rDOM consumption by HMA sponges could reproduce the observed patterns.

Based on the literature, we assume that sponges form an integral part of the food chain, leading to our hypothesis that sponges might reduce MeHg bioaccumulation in animals above them in the food web, including commercially important fish species.

https://doi.org/10.5194/egusphere-2025-5377
Preprint. Discussion started: 12 November 2025

The predicted 45% reduction in benthic fish MeHg concentrations represents a hypothesis-generating finding that demonstrates the potential magnitude of sponge-mediated effects. This should be interpreted as a loosely constrained upper bound estimate, given our generous parameterization of HMA sponge biomass and role in the food chain. The actual magnitude would depend on local sponge abundance, community structure, and food web dynamics. Both our mechanistic understanding of food web dynamics in the Bay of Villefranche and the role of sponges in them, and the dynamics between sponges and iHg should be validated with empirical studies before this estimation can be meaningfully constrained using sensitivity studies.

5.7 A potential role of sponges in bioremediation

Sponges are unique in their ability to bioaccumulate Hg, as they both have extremely high levels of iHg while maintaining very low levels of MeHg. This characteristic makes them a prime candidate for bioremediation studies. If the model is accurate for sponge grounds, they could be advantageous for Hg remediation. On the one hand, in Hg-polluted regions, sponges could bioaccumulate the less toxic iHg, which could then be extracted for bioremediation, with a diminished risk of MeHg since the majority of the Hg remains in its unmethylated form. Furthermore, the low MeHg content in HMA sponges means that organisms feeding on them would accumulate less MeHg, ultimately resulting in lower MeHg levels in higher trophic levels, as demonstrated in our model. These findings suggest that actively managing sponge grounds could both mitigate MeHg accumulation in fish and provide a sustainable method for extracting Hg from the marine environment.

6 Evaluate the hypotheses

We accept the hypothesis that **the consumption of DOM can explain the low MeHg content of LMA sponges, while a combination of consumption of DOM and demethylation explains the even lower concentration in HMA sponges**. We expand this by showing that while demethylation can play a role, DOM consumption can explain both the low MeHg concentration in LMA sponges, while the even lower concentration in HMA sponges can be explained by rDOM consumption or a demethylation rate of 1% d^{-1}.

We reject the hypothesis that **the consumption of DOM can explain the high iHg values of LMA and HMA sponges**. Even with an assimilation of 0.95 for iHg when DOM was consumed, our modeled iHg bioaccumulation was still an order of magnitude lower than observed. We demonstrate that the consumption of DOM can increase the iHg content in sponges, but to reproduce the iHg bioaccumulation, we need to assume that iHg is only released with respiration and not through an additional turnover or respiration rate, or that sponges have an elevated iHg uptake rate. We expand by providing an explanation of how we think that the binding of iHg to SPs in sponges can reduce the iHg from sponges.

We accept the final hypothesis that **sponges can lower the concentration of MeHg in fish**. We supplement this by showing a reduction of 45% in our model.

https://doi.org/10.5194/egusphere-2025-5377
Preprint. Discussion started: 12 November 2025

7 Summary and Conclusion

In this study, we modeled the benthic ecosystem of the Bay of Villefranche using the 1D GOTM-ECOSMO-MERCY coupled system. The simulated chlorophyll concentrations align with the NASA MODIS-A satellite time series. Pelagic iHg and MeHg concentrations are consistent with observations by Cossa et al. (2017), and MeHg bioaccumulation falls within the range reported by Llull et al. (2017); Tesán Onrubia et al. (2020). We ran the simulations assuming both that rDOM influences the ecosystem and Hg cycling, and assuming that rDOM is unreactive and does not play a key role. Our model and its comparison to the observations by Orani et al. (2020) demonstrate that several mechanisms could explain the observed Hg dynamics in Mediterranean sponges:

- DOM consumption provides a viable explanation for low MeHg in LMA sponges.
- The difference between MeHg bioaccumulation in LMA and HMA sponges can result from the consumption of rDOM by HMA sponges, or an *in vivo* demethylation rate of 1% d^{-1} in HMA sponges.
- The consumption of DOM by sponges contributes to elevated iHg levels, but this mechanism alone is insufficient to explain the extremely high iHg concentrations observed in both LMA and HMA sponges. This suggests that sponges either have increased uptake or a reduced release rate of iHg. We present evidence to support the hypothesis that the high iHg concentration in sponges is caused by a reduced release rate of iHg.
- As an alternative hypothesis, we demonstrate that if sponges have elevated iHg and MeHg uptake rates, a demethylation rate of 16% d^{-1} would be required, providing a loosely constrained upper bound for demethylation.

It must be noted that there is large unconstrained uncertainty in all results presented. This study should be seen as a hypothesis-generating modeling study rather than an exact quantification or verification of the proposed mechanisms. Targeted empirical research is needed to better understand the role of sponges in Hg cycling. However, based on our results, we propose that DOM-consuming sponges might play a key role in reducing MeHg bioaccumulation in benthic fish.

Conflict of interest

One of the authors is a member of the editorial board of biogeosciences.

Funding

This research has been funded by the European Union's Horizon 2020 research and innovation programme under the Marie Skłodowska-Curie grant agreement no. 860497.

https://doi.org/10.5194/egusphere-2025-5377
Preprint. Discussion started: 12 November 2025

8 Acknowledgments

Readability suggestions for this paper were generated using gAI tools such as ChatGPT (OpenAI), while AI-based spell checks such as Grammarly and Writefull were used to correct spelling. In addition, AI tools helped optimize the R and Python scripts and provide coding suggestions. All suggestions were implemented only after critical manual evaluation. Finally, Google Scholar and Perplexity were used to find sources for literature research, which were consequently manually read, verified, and cited. Several sub-images were generated that together compose the graphical abstract; these were generated using openART and GPT-4.1.

Code availability

The model code is publicly available on Zenodo (DOI: 10.5281/zenodo.17372353) under the GPL 3.0 License.

Author contributions

The contributions per author are listed in Table 6.

Table 6. Contributions per Author. Authors are: D. Amptmeijer (DA), Dr. U. Hanz (UH), Prof. Dr. C. Schrum (CS), and Dr. J. Bieser (JB).

Contributor role	Role definition	Authors
Conceptualisation	Conceptualized the study	DA, JB, UH, CS
	Developed the research objectives	DA, JB, UH, CS
Methodology	Implementation of the model into FABM	DA
	Identified the LMA or HMA sponges in the observational dataset	UH
	Developed the hGOTM tool required to build the physical setup of the model	JB
	Built the physical GOTM setup for the Bay of Villefranche	DA
Evaluation	Evaluated the model performance against observations	DA
	Performed statistical tests on the observations	DA
Writing	Writing of the original draft	DA
	Review of the original draft and quality control	UH, JB, DA
Funding acquisition	Acquired funding via the GMOS-Train ITN	JB

https://doi.org/10.5194/egusphere-2025-5377
Preprint. Discussion started: 12 November 2025

Appendix A: Equations for statistical metrics

A1.

Table A1. Formulas for statistical metrics used to evaluate model. x_i and y_i are the modeled and observed values, respectively, n is the number of data points, and $\bar{x}$ is the modeled mean and $\bar{y}$ the observed mean.

Metric	**Formula**
Root Mean Square Error (RMSE)	$\text{RMSE} = \sqrt{\frac{1}{n}\sum_{i=1}^{n}(x_i - y_i)^2}$
Pearson correlation coefficient r	$r = \frac{\sum_{i=1}^{n}(x_i-\bar{x})(y_i-\bar{y})}{\sqrt{\sum_{i=1}^{n}(x_i-\bar{x})^2}\sqrt{\sum_{i=1}^{n}(y_i-\bar{y})^2}}$
Standard deviation σ	$\sigma = \sqrt{\frac{1}{n}\sum_{i=1}^{n}(x_i - \bar{x})^2}$
Bias	$\text{Bias} = \frac{1}{n}\sum_{i=1}^{n}(x_i - y_i)$
Mean Percent Bias (MPB)	$\text{MPB} = 100 \times \frac{\bar{x}-\bar{y}}{\bar{y}}$

https://doi.org/10.5194/egusphere-2025-5377
Preprint. Discussion started: 12 November 2025

References

Amptmeijer, D. J., Bieser, J., Mikheeva, E., Daewel, U., and Schrum, C.: Bioaccumulation as a driver of high MeHg in coastal Seas, EGUsphere [preprint], https://doi.org/https://doi.org/10.5194/egusphere-2025-1486,2025., 2025a.

Amptmeijer, D. J., Padilla, A., Modesti, S., and Schrum, C.: Feeding strategy as a key driver of the bioaccumulation of MeHg in megabenthos, Under review in Biogeochemistry, 2025b.

Baltar, F., Alvarez-Salgado, X. A., Arístegui, J., Benner, R., Hansell, D. A., Herndl, G. J., and Lønborg, C.: What Is Refractory Organic Matter in the Ocean?, Frontiers in Marine Science, 8, https://doi.org/10.3389/fmars.2021.642637, 2021.

Bart, M. C., de Kluijver, A., Hoetjes, S., Absalah, S., Mueller, B., Kenchington, E., Rapp, H. T., and de Goeij, J. M.: Differential processing of dissolved and particulate organic matter by deep-sea sponges and their microbial symbionts, Scientific Reports 2020 10:1, 10, 1–13, https://doi.org/10.1038/s41598-020-74670-0, 2020.

Bart, M. C., Mueller, B., Rombouts, T., van de Ven, C., Tompkins, G. J., Osinga, R., Brussaard, C. P., MacDonald, B., Engel, A., Rapp, H. T., and de Goeij, J. M.: Dissolved organic carbon (DOC) is essential to balance the metabolic demands of four dominant North-Atlantic deep-sea sponges, Limnology and Oceanography, 66, 925–938, https://doi.org/10.1002/LNO.11652, 2021.

Belgacem, M., Schroeder, K., Barth, A., Troupin, C., Pavoni, B., Raimbault, P., Garcia, N., Borghini, M., and Chiggiato, J.: Climatological distribution of dissolved inorganic nutrients in the western Mediterranean Sea (1981-2017), Earth System Science Data, 13, 5915–5949, https://doi.org/10.5194/ESSD-13-5915-2021, 2021.

Bellanger, M., Pichery, C., Aerts, D., Berglund, M., Castaño, A., Čejchanová, M., Crettaz, P., Davidson, F., Esteban, M., Fischer, M. E., Gurzau, A. E., Halzlova, K., Katsonouri, A., Knudsen, L. E., Kolossa-Gehring, M., Koppen, G., Ligocka, D., Miklavčič, A., Reis, M. F., Rudnai, P., Tratnik, J. S., Weihe, P., Budtz-Jorgensen, E., and Grandjean, P.: Economic benefits of methylmercury exposure control in Europe: monetary value of neurotoxicity prevention, Environmental health : a global access science source, 12, https://doi.org/10.1186/1476-069X-12-3, 2013.

Bertolino, M., Reboa, A., Armenio, C., Castellano, M., Felline, S., Terlizzi, A., and Bavestrello, G.: Sponges as feeding resource for the white seabream Diplodus sargus (Linnaeus, 1758) from the Mediterranean Sea, The European Zoological Journal, 91, 1192–1198, https://doi.org/10.1080/24750263.2024.2431084, 2024.

Bieser, J., Amptmeijer, D., Daewel, U., Kuss, J., Soerenson, A. L., and Schrum, C.: The 3D biogeochemical marine mercury cycling model MERCY v2.0; linking atmospheric Hg to methyl mercury in fish, Geoscientific Model Development Discussions, pp. 1–59, https://doi.org/10.5194/GMD-2021-427, 2023.

Bolding, K., Bruggeman, J., Burchard, H., and Umlauf, L.: General Ocean Turbulence Model - GOTM, https://doi.org/10.5281/ZENODO.4896611, 2021.

Bruggeman, J. and Bolding, K.: A general framework for aquatic biogeochemical models, Environmental Modelling & Software, 61, 249–265, https://doi.org/10.1016/J.ENVSOFT.2014.04.002, 2014.

Claisse, D.: Chemical Contamination of French Coasts The Results of a Ten Years Mussel Watch, Marine Pollution Bulletin, 1989.

Cossa, D., Durrieu de Madron, X., Schäfer, J., Lanceleur, L., Guédron, S., Buscail, R., Thomas, B., Castelle, S., and Naudin, J. J.: The open sea as the main source of methylmercury in the water column of the Gulf of Lions (Northwestern Mediterranean margin), Geochimica et Cosmochimica Acta, 199, 222–237, https://doi.org/10.1016/J.GCA.2016.11.037, 2017.

https://doi.org/10.5194/egusphere-2025-5377
Preprint. Discussion started: 12 November 2025

Cresson, P., Travers-Trolet, M., Rouquette, M., Timmerman, C. A., Giraldo, C., Lefebvre, S., and Ernande, B.: Underestimation of chemical contamination in marine fish muscle tissue can be reduced by considering variable wet:dry weight ratios, Marine Pollution Bulletin, 123, 279–285, https://doi.org/10.1016/j.marpolbul.2017.08.046, 2017.

Cruz, K., Guézennec, J., and Barkay, T.: Binding of Hg by bacterial extracellular polysaccharide: a possible role in Hg tolerance, Applied Microbiology and Biotechnology, 101, 5493–5503, https://doi.org/10.1007/s00253-017-8239-z, 2017.

Cushing, D. H.: The estimation of carbon in phytoplankton, Rappt. Proces-Verbaux Reunions, Conseil Perm. Intern. Exploration Mer, 144, 32–33, 1958.

da Cruz, J. F., Gaspar, H., and Calado, G.: Turning the game around: Toxicity in a nudibranch-sponge predator-prey association, Chemoecology, 22, 47–53, https://doi.org/10.1007/S00049-011-0097-Z/FIGURES/4, 2012.

Daewel, U. and Schrum, C.: Simulating long-term dynamics of the coupled North Sea and Baltic Sea ecosystem with ECOSMO II: Model description and validation, Journal of Marine Systems, 119-120, 30–49, https://doi.org/10.1016/J.JMARSYS.2013.03.008, 2013.

Daewel, U., Schrum, C., and MacDonald, J. I.: Towards end-to-end (E2E) modelling in a consistent NPZD-F modelling framework (ECOSMO E2E-v1.0): Application to the North Sea and Baltic Sea, Geoscientific Model Development, 12, 1765–1789, https://doi.org/10.5194/gmd-12-1765-2019, 2019.

De Goeij, J. M., Van Oevelen, D., Vermeij, M. J., Osinga, R., Middelburg, J. J., De Goeij, A. F., and Admiraal, W.: Surviving in a marine desert: The sponge loop retains resources within coral reefs, Science, 342, 108–110, https://doi.org/10.1126/SCIENCE.1241981/SUPPL_FILE/DE.GOEIJ.SM.PDF, 2013.

Dolan, J. R.: The History of Biological Exploration of the Bay of Villefranche, Protist, 165, 636–644, https://doi.org/10.1016/J.PROTIS.2014.07.005, 2014.

Dutton, J. and Fisher, N. S.: Bioavailability of sediment-bound and algal metalsto killifish Fundulus heteroclitus, Aquatic biology, 16, 85–96, 2012.

Erwin, P. M., Coma, R., Serrano, E., and Ribes, M.: Stable symbionts across the HMA-LMA dichotomy: low seasonal and interannual variation in sponge-associated bacteria from taxonomically diverse hosts, FEMS Microbiology Ecology, 91, https://doi.org/10.1093/femsec/fiv115, 2015.

Esteves, A. I., Nicolai, M., Humanes, M., and Goncalves, J.: Sulfated polysaccharides in marine sponges: Extraction methods and anti-HIV activity, Marine Drugs, 9, 139–153, https://doi.org/10.3390/md9010139, 2011.

Fonds, M., Cronie, R., Vethaak, A. D., and Van Der Puyl, P.: Metabolism, food consumption and growth of plaice (Pleuronectes platessa) and flounder (Platichthys flesus) in relation to fish size and temperature, Netherlands Journal of Sea Research, 29, 127–143, https://doi.org/10.1016/0077-7579(92)90014-6, 1992.

Fromentin, J.-M., Dauvin, J.-C., Ibanez, F., Dewarumez, J.-M., and Elkaim, B.: Long-term variations Macrobenthos Community structure, Tech. rep., 1997.

Garcia-Arevalo, I., Berard, J.-B., Bieser, J., Le Faucheur, S., Hubert, C., Lacour, T., Thomas, B., Cossa, D., and Knoery, J.: Mercury Accumulation Pathways in a Model Marine Microalgae: Sorption, Uptake, and Partition Kinetics, https://doi.org/10.1021/acsestwater.3c00795, 2024.

García-Bonilla, E., Brandão, P. F. B., Thierry Pérez, ., and Junca, H.: Stable and Enriched Cenarchaeum symbiosum and Uncultured Betaproteobacteria HF1 in the Microbiome of the Mediterranean Sponge Haliclona fulva (Demospongiae: Haplosclerida), ENVIRONMENTAL MICROBIOLOGY, pp. 25–36, https://doi.org//10.1007/s00248-018-1201-5, 2019.

https://doi.org/10.5194/egusphere-2025-5377
Preprint. Discussion started: 12 November 2025

Garcia H.E., Boyer T.P., Baranova O.K., Locarnini R.A., Mishonov A.V., Grodsky A., Paver C.R., Weathers K.W., Smolyar I.V., Reagan J.R., Seidov D., and Zweng M.W.: World Ocean Atlas 2018: Product Documentation. A. Mishonov, Technical Editor., 2019.

GEBCO Bathymetric Compilation Group: The GEBCO_2020 Grid - a continuous terrain model of the global oceans and land., Tech. rep., https://doi.org//10.5285/a29c5465-b138-234d-e053-6c86abc040b9, 2020.

Gloeckner, V., Wehrl, M., Moitinho-Silva, L., Gernert, C., Schupp, P., Pawlik, J. R., Lindquist, N. L., Erpenbeck, D., Wo¨rheide, G., Wo¨rheide, W., and Hentschel, U.: The HMA-LMA Dichotomy Revisited: an Electron Microscopical Survey of 56 Sponge Species, Tech. rep., 2014.

Hanz, U., Riekenberg, P., De Kluijver, A., Van Der Meer, M., Jack, ., Middelburg, J., Jasper, ., De Goeij, M., Martijn, ., Bart, C., Wurz, E., Colaço, A., Gerard, ., Duineveld, C. A., Reichart, G.-J., Rapp, . H.-T., and Mienis, F.: The important role of sponges in carbon and nitrogen cycling in a deep-sea biological hotspot, https://doi.org/10.1111/1365-2435.14117, 2022.

Hentschel, U., Usher, K. M., and Taylor, M. W.: Marine sponges as microbial fermenters, FEMS Microbiol Ecol, 55, 167–177, https://doi.org/10.1111/j.1574-6941.2005.00046.x, 2006.

Hentschel, U., Piel, J., Degnan, S. M., and Taylor, M. W.: Genomic insights into the marine sponge microbiome, Nature Reviews Microbiology, 10, 641–654, https://doi.org/10.1038/NRMICRO2839, 2012.

Jeong, H., Ali, W., Zinck, P., Souissi, S., and Lee, J. S.: Toxicity of methylmercury in aquatic organisms and interaction with environmental factors and coexisting pollutants: A review, Science of the Total Environment, 943, https://doi.org/10.1016/j.scitotenv.2024.173574, 2024.

Koopmans, M. and Wijffels, R. H.: Seasonal Growth Rate of the Sponge Haliclona oculata (Demospongiae: Haplosclerida), Marine Biotechnology (New York, N.y.), 10, 502, https://doi.org/10.1007/S10126-008-9086-9, 2008.

Labrune, C., Grémare, A., Amouroux, J. M., Sardá, R., Gil, J., and Taboada, S.: Assessment of soft-bottom polychaete assemblages in the Gulf of Lions (NW Mediterranean) based on a mesoscale survey, Estuarine, Coastal and Shelf Science, 71, 133–147, https://doi.org/10.1016/J.ECSS.2006.07.007, 2007.

Lavoie, R. A., Jardine, T. D., Chumchal, M. M., Kidd, K. A., and Campbell, L. M.: Biomagnification of Mercury in Aquatic Food Webs: A Worldwide Meta-Analysis, https://doi.org/10.1021/es403103t, 2013.

Lee, C. S. and Fisher, N. S.: Methylmercury uptake by diverse marine phytoplankton, Limnology and Oceanography, 61, 1626–1639, https://doi.org/10.1002/lno.10318, 2016.

Llull, R. M., Garí, M., Canals, M., Rey-Maquieira, T., and Grimalt, J. O.: Mercury concentrations in lean fish from the Western Mediterranean Sea: Dietary exposure and risk assessment in the population of the Balearic Islands, Environmental Research, 158, 16–23, https://doi.org/10.1016/j.envres.2017.05.033, 2017.

Lønborg, C., Carreira, C., Abril, G., Agustí, S., Amaral, V., Andersson, A., Arístegui, J., Bhadury, P., Bif, M. B., Borges, A. V., Bouillon, S., Calleja, M. L., Cotovicz, L. C., Cozzi, S., Doval, M., Duarte, C. M., Eyre, B., Fichot, C. G., García-Martín, E. E., Garzon-Garcia, A., Giani, M., Gonçalves-Araujo, R., Gruber, R., Hansell, D. A., Hashihama, F., He, D., Holding, J. M., Hunter, W. R., Ibánhez, J. S. P., Ibello, V., Jiang, S., Kim, G., Klun, K., Kowalczuk, P., Kubo, A., Lee, C. W., Lopes, C. B., Maggioni, F., Magni, P., Marrase, C., Martin, P., McCallister, S. L., McCallum, R., Medeiros, P. M., Morán, X. A. G., Muller-Karger, F. E., Myers-Pigg, A., Norli, M., Oakes, J. M., Osterholz, H., Park, H., Lund Paulsen, M., Rosentreter, J. A., Ross, J. D., Rueda-Roa, D., Santinelli, C., Shen, Y., Teira, E., Tinta, T., Uher, G., Wakita, M., Ward, N., Watanabe, K., Xin, Y., Yamashita, Y., Yang, L., Yeo, J., Yuan, H., Zheng, Q., and Álvarez-Salgado, X. A.: A global database of dissolved organic matter (DOM) concentration measurements in coastal waters (CoastDOM v1), Earth System Science Data, 16, 1107–1119, https://doi.org/10.5194/ESSD-16-1107-2024, 2024.

https://doi.org/10.5194/egusphere-2025-5377
Preprint. Discussion started: 12 November 2025

Maldonado, M. and Uriz, M. J.: Microrefuge exploitation by subtidal encrusting sponges: patterns of settlement and post-settlement survival, MARINE ECOLOGY PROGRESS SERIES Mar Ecol Prog Ser, 174, 141–150, 1998.

Mason, R. P., Reinfelder, J. R., and Morel, F. M.: Bioaccumulation of mercury and methylmercury, Water, Air, and Soil Pollution 1995 80:1, 80, 915–921, https://doi.org/10.1007/BF01189744, 1995.

Mason, R. P., Reinfelder, J. R., and Morel, F. M.: Uptake, toxicity, and trophic transfer of mercury in a coastal diatom, Environmental Science and Technology, 30, 1835–1845, https://doi.org/10.1021/es950373d, 1996.

Mathema, V. B., Thakuri, B. C., and Sillanpää, M.: Bacterial mer operon-mediated detoxification of mercurial compounds: A short review, https://doi.org/10.1007/s00203-011-0751-4, 2011.

Morel, F. M. M., Kraepiel, A. M. L., and Amyot, M.: The Chemical Cycle and Bioaccumulation of Mercury, Source: Annual Review of Ecology and Systematics, 29, 543–566, https://www.jstor.org/stable/221718?seq=1&cid=pdf-, 1998.

Orani, A. M., Vassileva, E., Azemard, S., and Thomas, O. P.: Comparative study on Hg bioaccumulation and biotransformation in Mediterranean and Atlantic sponge species, Chemosphere, 260, 127 515, https://doi.org/10.1016/J.CHEMOSPHERE.2020.127515, 2020.

Pacyna, E. G., Pacyna, J. M., Steenhuisen, F., and Wilson, S.: Global anthropogenic mercury emission inventory for 2000, Atmospheric Environment, 40, 4048–4063, https://doi.org/10.1016/j.atmosenv.2006.03.041, 2006.

Pan, K. and Wang, W. X.: Mercury accumulation in marine bivalves: Influences of biodynamics and feeding niche, Environmental Pollution, 159, 2500–2506, https://doi.org/10.1016/J.ENVPOL.2011.06.029, 2011.

Perger, R. and Temming, A.: A new method to determine in situ growth rates of decapod shrimp: A case study with brown shrimp Crangon crangon, Marine Biology, 159, 1209–1222, https://doi.org/10.1007/s00227-012-1901-1, 2012.

Regnault, M.: Journal of Comparative Physiology. B Respiration and Ammonia Excretion of the Shrimp Crangon crangon L.: Metabolic Response to Prolonged Starvation, J. Comp. Physiol, 141, 549–555, https://doi.org//10.1007/BF01101478, 1981.

REPHY: Time Series: REPHY Villefranche, https://www.st.nmfs.noaa.gov/copepod/time-series/fr-50114/, https://www.st.nmfs.noaa.gov/copepod/time-series/fr-50114/, 2020.

Ribes, M., Coma, R., Research, J. G. J. o. P., and 1999, u.: Seasonal variation of particulate organic carbon, dissolved organic carbon and the contribution of microbial communities to the live particulate organic carbon in a shallow near-bottom ecosystem at the Northwestern Mediterranean Sea, Journal of Plankton Research, 21, 1077–1100, https://academic.oup.com/plankt/article-abstract/21/6/1077/1479175, 1999.

Ricciardi, A. and Bourget, E.: Weight-to-weight conversion factors for marine benthic macroinvertebrates, Marine ecology progress series, 163, 245–251, 1998.

Rijsgard, H. and Banta, G.: Irrigation and deposit feeding by the lugworm Arenicula marina, characteristics and secondary effects on the environment. A review of current knowledge., Vie et Milieu / Life & Environment, 4, 243–257, https://hal.sorbonne-universite.fr/hal-03173003, 1998.

Rodil, I. F., Attard, K. M., Norkko, J., Glud, R. N., and Norkko, A.: Estimating Respiration Rates and Secondary Production of Macrobenthic Communities Across Coastal Habitats with Contrasting Structural Biodiversity, https://doi.org/10.1007/s10021-019-00427-0, 2019.

Rosenberg, R., Gre´maregre´mare, A., Amouroux, J.-M., and Nilsson, H. C.: Benthic habitats in the northwest Mediterranean characterised by sedimentary organics, benthic macrofauna and sediment profile images, Estuarine, Coastal and Shelf Science, pp. 297–311, https://doi.org/10.1016/S0272-7714(02)00356-6, 2003.

Santos-Gandelman, J. F., Giambiagi-Demarval •, M., Muricy, G., Barkay, T., and Laport, M. S.: Mercury and methylmercury detoxification potential by sponge-associated bacteria, Antonie van Leeuwenhoek, pp. 585–590, https://doi.org/10.1007/s10482-014-0224-2, 2014.

https://doi.org/10.5194/egusphere-2025-5377
Preprint. Discussion started: 12 November 2025

Schartup, A. T., Ndu, U., Balcom, P. H., Mason, R. P., and Sunderland, E. M.: Contrasting Effects of Marine and Terrestrially Derived Dissolved Organic Matter on Mercury Speciation and Bioavailability in Seawater, https://doi.org/10.1021/es506274x, 2015.

Seelen, E., Liem-Nguyen, V., Wünsch, U., Baumann, Z., Mason, R., Skyllberg, U., and Björn, E.: Dissolved organic matter thiol concentrations determine methylmercury bioavailability across the terrestrial-marine aquatic continuum, Nature Communications, 14, https://doi.org/10.1038/s41467-023-42463-4, 2023.

Storelli, M. M., Stuffler, R. G., and Marcotrigiano, G. O.: Total and methylmercury residues in tuna-fish from the Mediterranean sea, Food Additives and Contaminants, 19, 715–720, https://doi.org/10.1080/02652030210153569, 2002.

Tesán Onrubia, J. A., Petrova, M. V., Puigcorbé, V., Black, E. E., Valk, O., Dufour, A., Hamelin, B., Buesseler, K. O., Masqué, P., Le Moigne, F. A., Sonke, J. E., Rutgers Van Der Loeff, M., and Heimbürger-Boavida, L. E.: Mercury Export Flux in the Arctic Ocean Estimated from 234Th/238U Disequilibria, ACS Earth and Space Chemistry, 4, 795–801, https://doi.org/10.1021/acsearthspacechem.0c00055, 2020.

Tesán-Onrubia, J. A., Heimbürger-Boavida, L. E., Dufour, A., Harmelin-Vivien, M., García-Arévalo, I., Knoery, J., Thomas, B., Carlotti, F., Tedetti, M., and Bănaru, D.: Bioconcentration, bioaccumulation and biomagnification of mercury in plankton of the Mediterranean Sea, Marine Pollution Bulletin, 194, 115 439, https://doi.org/10.1016/J.MARPOLBUL.2023.115439, 2023.

Thiel, V., Leininger, S., Schmaljohann, R., Brümmer, F., and Imhoff, J. F.: Sponge-specific Bacterial Associations of the Mediterranean Sponge Chondrilla nucula (Demospongiae, Tetractinomorpha), Microbial Ecology, 54, 101–111, https://doi.org/10.1007/s00248-006-9177-y, 2007.

Thomassen, S. and Riisgadrd, H. U.: Growth and energetics of the sponge Halichondria panicea, 128, 239–246, 1995.

Tseng, C.-M., Ang, S.-J., Chen, Y.-S., Shiao, J.-C., Lamborg, C. H., He, X., and Reinfelder, J. R.: Bluefin tuna reveal global patterns of mercury pollution and bioavailability in the world's oceans, PNAS, 118, https://doi.org//10.1073/pnas.211120, 2021.

Tsui, M. T. and Wang, W. X.: Uptake and Elimination Routes of Inorganic Mercury and Methylmercury in Daphnia magna, Environmental Science and Technology, 38, 808–816, https://doi.org/10.1021/es034638x, 2004.

Vacelet, J. and Donadey, C.: Electron microscope study of the association between some sponges and bacteria, Journal of Experimental Marine Biology and Ecology, 30, 301–314, https://doi.org/10.1016/0022-0981(77)90038-7, 1977.

Vilanova, E., Zilberberg, C., Kochem, M., Custodio, M. R., and Mourão, P. A. S.: A novel biochemical method to distinguish cryptic species of Chondrilla (Chondrosida, Demospongiae) based on its sulfated polysaccharides, Porifera research : Biodiversity , innovation and sustainaBility, pp. 653–659, https://www.researchgate.net/profile/Marcio-Custodio-2/publication/257954142_Porifera_Research_Biodiversity_Innovation_and_Sustainability/links/0deec526798bb07302000000/Porifera-Research-Biodiversity-Innovation-and-Sustainability.pdf#page=663, 2007.

Vogel, S.: Current-induced flow through the sponge, Halichondria., Tech. rep., 1974.

Wallace, J. C.: Feeding, Starvation and Metabolic Rate in the Shore Crab Carcinus maenas, Marine Biology, 20, 227–281, 1973.

Webster, N. S. and Thomas, T.: The sponge hologenome, mBio, 7, 135–151, https://doi.org/10.1128/MBIO.00135-16/ASSET/D04245CF-8B86-46F5-B77D-681D219589C5/ASSETS/GRAPHIC/MBO0021628090002.JPEG, 2016.

Weisz, J. B., Lindquist, N., and Martens, C. S.: Do associated microbial abundances impact marine demosponge pumping rates and tissue densities?, Oecologia, 155, 367–376, https://doi.org/10.1007/S00442-007-0910-0/FIGURES/4, 2008.

Wouters, H., Berckmans, J., Maes, R., Vanuytrecht, E., and De Ridder, K.: Global bioclimatic indicators from 1979 to 2018 derived from reanalysis, version 1.0, Copernicus Climate Change Service (C3S) Climate Data Store (CDS), DOI: 10.24381/cds.bce175f0, 2021.